

Total Synthesis, Characterization, and Conformational Analysis of the Naturally-Occurring Hexadecapeptide Integramide A and Its Diastereomer at Positions 14 and 15

Marta De Zotti,^[a] Francesca Damato,^[a] Fernando Formaggio,^[a] Marco Crisma,^[a] Elisabetta Schievano,^[a] Stefano Mammi,^[a] Bernard Kaptein,^[b] Quirinus B. Broxterman,^[b] Peter J. Felock,^[c] Daria J. Hazuda,^[c] Sheo B. Singh,^[c] Jochen Kirschbaum,^[d] Hans Brückner,^[d] and Claudio Toniolo*^[a]

Dedicated to the Centenary of the Italian Chemical Society and to the memory of Professor Ernesto Scoffone, founder of peptide chemistry in Italy and a great mentor.

Abstract: Integramide A is a 16 amino acid peptide inhibitor of the enzyme HIV-1 integrase. We have recently reported that the chiralities of the dipeptide sequence near the C-terminus are L-Iva¹⁴-D-Iva¹⁵. Here, we describe the syntheses in solution of the natural compound and its D-Iva¹⁴-L-Iva¹⁵ diastereomer and the results of their

chromatographic / mass spectrometric characterizations. The conformational analysis is presented of the two compounds and some of their synthetic intermediates of different main-chain length in the crystal state (by X-ray diffraction) and in solvents of different polarities (using CD, FT-IR absorption, and 2D NMR techniques). These data

provide useful information to shed light on the mechanism of inhibition of HIV-1 integrase, an important target for anti-HIV therapy.

Keywords: circular dichroism • IR spectroscopy • NMR spectrometry • peptide synthesis • X-ray diffraction

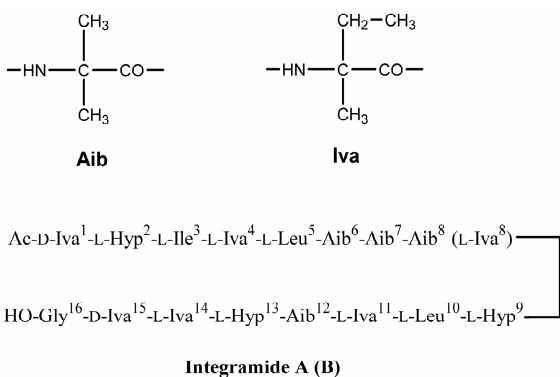
Introduction

Human immunodeficiency virus type 1 (HIV-1), like all retroviruses, depends upon the integration of a DNA copy of its viral genome into the host cell chromosomes as part of its infection cycle. Multiple steps in this integration process are catalyzed by the enzyme HIV-1 integrase. The integration of HIV-1 DNA into the host chromosome is achieved by the integrase protein performing a series of DNA cutting and joining reactions.

Integrase is an attractive target for anti-HIV therapy because it is essential for virus replication and, unlike protease and reverse transcriptase, there are no known counterparts in the host cell. Furthermore, integrase takes advantage of a single active site to accommodate two different conformations of DNA substrates, which may constrain the ability of HIV to develop drug resistance to integrase inhibitors.^[1] A variety of classes of HIV-integrase inhibitors is known,^[2] including some non-Aib (α -aminoisobutyric acid) / Iva (isovaline) peptides of modest activity.^[3] However, a recent publication from three of the authors of this paper (S.B.S., P.J.F., and D.J.H.) has dealt with two naturally-occurring, non-ribosomal peptide molecules (integramides A and B) which exhibit significant inhibitory activities.^[4]

- [a] Dr. M. De Zotti, F. Damato, Prof. F. Formaggio, Dr. M. Crisma, Dr. E. Schievano, Prof. S. Mammi, Prof. C. Toniolo
Institute of Biomolecular Chemistry, CNR, Padova Unit, Department of Chemistry, University of Padova
via Marzolo 1, 35131 Padova, Italy
Fax: (+39) 049-827-5239
E-mail: claudio.toniolo@unipd.it
- [b] Dr. B. Kaptein, Dr. Q.B. Broxterman
DSM Pharmaceutical Products
Innovative Synthesis and Catalysis, P.O. Box 18
6160 MD Geleen, The Netherlands
- [c] Dr. P.J. Felock, Dr. D.J. Hazuda, Dr. S.B. Singh
Merck Research Laboratories
Rahway, NJ 07065 and West Point, PA 19486, U.S.A.
- [d] Dr. J. Kirschbaum, Prof. H. Brückner
Department of Food Sciences, Interdisciplinary Research Centre for Biosystems, Land Use and Nutrition
University of Giessen
35392 Giessen, Germany

Supporting information for this article is available on the WWW under <http://www.chemeurj.org/> or from the author.



Integramides are linear peptides, 16 amino acid long and rich in Aib and Iva residues. There are four Aib and five Iva residues in the sequence of integramide A, and three Aib and six Iva residues in integramide B: integramide A has an Aib residue at position 8, while its B analogue has an L-Iva residue at the same position. While their C-terminus is free, their N-terminus is acetylated (Ac). In the initial work,^[4] the absolute configuration of the two consecutive C-terminal -Iva¹⁴-Iva¹⁵- residues could not be determined, although it was known that one is L and the other is D. More recently, using HPLC and NMR techniques and the two L-Iva¹⁴-D-Iva¹⁵ and D-Iva¹⁴-L-Iva¹⁵ synthetic diastereomeric hexadecapeptides, we were able to elucidate this originally unsettled stereochemical problem, providing unambiguous evidence that the natural inhibitors contain the L-Iva¹⁴-D-Iva¹⁵ chiral pair.^[5] We also showed that the stereochemical inversion in the Iva¹⁴-Iva¹⁵ natural sequence is in general not detrimental and might be even slightly beneficial for activity against the strand transfer reaction.

In the present article we describe in great detail the strategy we used in solution for the challenging synthesis of the two diastereomeric 16-mers and their extensive characterization using HPLC, chiral chromatography, and mass spectrometry (MS) analyses. The results of an in-depth conformational investigation of the two hexadecapeptides and some of their short-sequence synthetic intermediates using X-ray diffraction, CD, FT-IR absorption and NMR techniques are also presented. In our previous communication on these compounds,^[5] only the results of the configurational study were reported, but neither the synthetic approach and the related analytical data nor the conformational findings were discussed. A very preliminary NMR conformational investigation of integramide A was already published^[4] but, as opposed to the helix-supporting solvent used in this work (TFE-*d*₂, deuterated 2,2,2-trifluoroethanol), it was performed in a solvent (deuterated pyridine) not entirely appropriate for such an analysis because of its known tendency to interact with the H-bonding donor (peptide) NH groups.

Results and Discussion

Synthesis and Characterization. For the large-scale production of enantiomerically pure L-Iva and D-Iva, an economically attractive and generally applicable chemo-enzymatic synthesis developed by DSM was used.^[6] It involves a combination of organic synthesis for the preparation of the racemic α -amino amides, followed by the exploitation of a broadly specific α -amino amidase to achieve optical resolution.

The segment condensation strategy adopted for the synthesis of the two diastereomeric (L-Iva¹⁴-D-Iva¹⁵ and D-Iva¹⁴-L-Iva¹⁵) hexadecapeptides in solution is illustrated in *Scheme 1*. The three

planned segments **B**, **C**, and **D** are of similar length. They avoid Aib(Iva)-Hyp [Hyp is (2*S*,4*R*)-4-hydroxyproline] dipeptide sequences, which are acid labile and prone to undergo intramolecular cyclization to 2,5-dioxopiperazine when located at the N-terminus, and prevent epimerization in the coupling reaction due to the absence of chiral C ^{α} -trisubstituted amino acids in the last and penultimate positions of the chain.^[7] Indeed, any C-activation of amino acid derivatives and peptide segments, such as **A**, **B**, and **C**, with their C-terminal C ^{α} -tetrasubstituted amino acid (Iva or Aib), is known to produce an otherwise easily epimerizable 5(4*H*)-oxazolone intermediate to a considerable extent.

For the formation of the difficult peptide bonds, in particular those connecting either two sterically demanding C ^{α} -tetrasubstituted amino acids (Aib / Iva) or one of them followed by an N-alkylated Hyp residue,^[7] the carboxyl group of the N ^{α} -protected amino acid or peptide was activated with the N-ethyl-N'-(3-dimethylaminopropyl)carbodiimide (EDC) / 7-aza-1-hydroxy-1,2,3-benzotriazole (HOAt) method.^[8] The poorly reactive, secondary alcoholic functionalities in the side chains of the Hyp residues were used without protection. The C-terminal *Or*Bu carboxylic ester protection was removed by the classical trifluoroacetic acid method in segments **B** and **C**, lacking any Aib(Iva)-Hyp bond, whereas a mildly acidic fluoroalcohol, 1,1,1,3,3,3-hexafluoroacetone hydrate, was used to afford the final **A-B-C-D** hexadecapeptide.^[9]

The HPLC profiles shown in Figure 1 demonstrate the purity of the two Ac/OH hexadecapeptide diastereomers. As reported in ref. [5], the chromatographic behavior of natural integramide A is identical to that of the L-Iva¹⁴-D-Iva¹⁵ diastereomer, but differs significantly from that of the D-Iva¹⁴-L-Iva¹⁵ diastereomer.

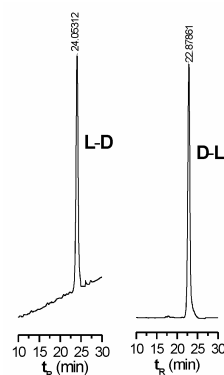
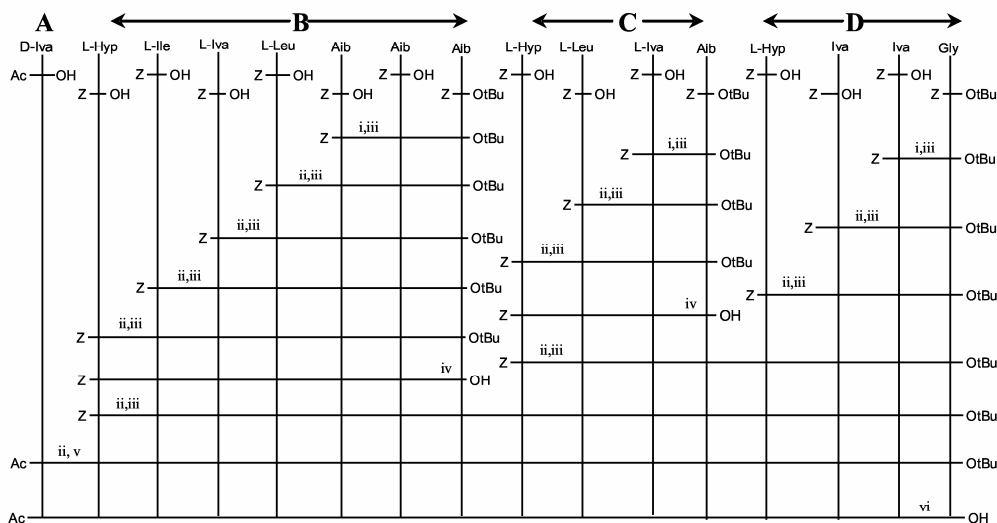


Figure 1. HPLC profiles for the two synthetic hexadecapeptide diastereomers L-Iva¹⁴-D-Iva¹⁵ (**L-D**) and D-Iva¹⁴-L-Iva¹⁵ (**D-L**). Conditions: analytical Phenomenex Kromasil C₁₈ column (particle size: 5 μ m; pore size: 100 \AA); gradient system: 65% to 80% B in 30 min; eluant A, 9:1 H₂O and 0.05% trifluoroacetic acid (TFA) / CH₃CN; eluant B: 9:1 CH₃CN / H₂O and 0.05% TFA; flow rate: 1 mL/min; room temperature; absorbance detector at 226 nm.

A total acid hydrolyzate of each of the two synthetic hexadecapeptide diastereomers was derivatized with Marfey's reagent according to the literature procedure.^[10] The L-Iva (eluted at 27.9 min) and D-Iva (eluted at 30.3 min) enantiomers were baseline resolved by HPLC. The average L-Iva/D-Iva ratio obtained (two analyses for each sample) was 1.48 (\pm 0.03) for the L-Iva¹⁴-D-Iva¹⁵ hexadecapeptide and 1.43 (\pm 0.03) for the D-Iva¹⁴-L-Iva¹⁵ hexadecapeptide.^[4] These two experimental values should be compared with the calculated ratio (3 L-Iva and 2 D-Iva) of 1.50. A synthetic, racemic D,L-Iva amino acid, used as a standard, gave the expected L/D ratio (1.00).



Scheme 1. Strategy adopted for the synthesis of the two hexadecapeptide diastereomers Ac/OH **A-B-C-D**[Hyp^{2,9,13}], (-D-Iva¹⁴-L-Iva¹⁵-) and (-L-Iva¹⁴-D-Iva¹⁵-). (i): H₂/Pd in distilled CH₂Cl₂; (ii): H₂/Pd in MeOH; (iii): EDC and HOAt (1.3 equiv. each) in distilled CH₂Cl₂, keeping the pH at 8 by adding N-methylmorpholine (NMM); (iv) trifluoroacetic acid (10 equiv.) in CH₂Cl₂; (v) EDC, HOAt, and Ac-D-Iva-OH (15 equiv. each) in DMF (N,N-dimethylformamide), keeping the pH at 8 by adding NMM; (vi) 1,1,1,3,3,3-hexafluoroacetone hydrate.

Total acid hydrolyzates of natural integramide **A** and the synthetic L-Iva¹⁴-D-Iva¹⁵ hexadecapeptide were separately converted into N^α-trifluoroacetyl-amino acid 2-propyl esters. The resulting derivatives were resolved on a Chirasil-L-Val capillary column and analyzed by selected-ion monitoring (SIM) MS. The presence of Aib, Gly, L-Leu, L-Ile, and L-Hyp was detected. Moreover, the derivatives of L-Iva and D-Iva, satisfactorily resolved, provided L-Iva/D-Iva ratios of 1.48 (natural compound) and 1.42 (synthetic compound). Trace amounts of D-Leu in the natural compound (1.8%) and in the synthetic compound (3.8%) are attributed to minor sequence-dependent racemization during acid hydrolysis and epimerization during the coupling steps in the peptide synthesis.

The ESI-CID (collision induced dissociation)-MS of the synthetic L-Iva¹⁴-D-Iva¹⁵ hexadecapeptide (Figure 2) shows the intense peak of the sodium adduct of the molecular ion at m/z 1653.9 as well as a regular series of $b_3 - b_8$ acylium ions at m/z 368.0, 467.0, 580.0, 665.2, 750.2, and 835.3, resulting from the sequence Ac-Iva-Hyp-Ile³-Iva-Leu-Aib-Aib-Aib⁸⁺. Ions b_{11} and b_{14} at m/z 1160.3 and 1457.3, respectively, are of very low abundance, whereas ions b_{12} and b_{15} at m/z 1245.3 and 1556.3, respectively, are remarkably intense. The high intensity of the b_8 and b_{12} ions is related to the preferred cleavage of the Aib⁸-Hyp⁹ and Aib¹²-Hyp¹³ peptide bonds.^[10] In the CID-off mode, the fragment ions b_9 , b_{10} , and b_{13} are not generated (but they are formed when CID 50 % is applied, not shown). The a_2 fragment ion at m/z 226.9 results from loss of CO from the b_2 ion. An ion denoted x_4 at m/z 411.0 represents the protonated internal tetrapeptide fragment ion Hyp⁹-Leu-Iva-Aib¹². Loss of the C-terminal Aib therefore is assumed to generate the ion at m/z 326.0. The ESI-CID -MS of the synthetic L-Iva¹⁴-D-Iva¹⁵ hexadecapeptide (Figure 2) and that of natural integramide **A** show almost perfect agreement.

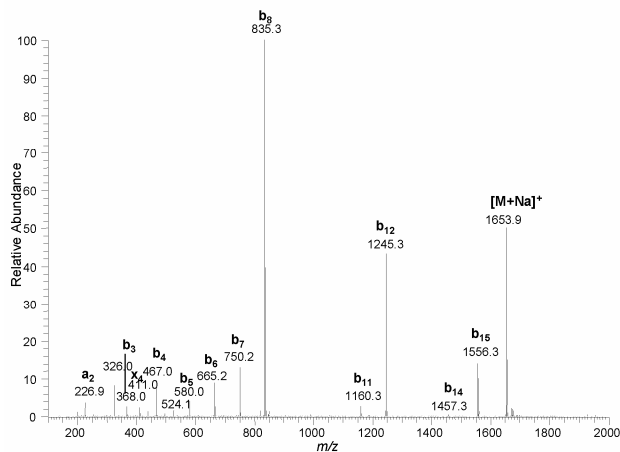


Figure 2. Positive ion ESI-MS for the synthetic L-Iva¹⁴-D-Iva¹⁵ hexadecapeptide.

Crystal-state Conformational Analysis. Despite a number of attempts, we were unable to grow a single crystal from any of the two hexadecapeptide diastereomers. However, we succeeded in preparing crystals suitable for X-ray diffraction from four terminally-protected segments of integramide **A** or its D-Iva-L-Iva diastereomer: (i) Z-D-Iva-L-Iva-Gly-OrBu (Z, benzyloxycarbonyl; OrBu, *tert*-butoxy), the C-terminal tripeptide of segment **D**, already described in ref. [11]; (ii) Z-L-Hyp-L-Iva-D-Iva-Gly-OrBu, a tetrapeptide which spans the full sequence of segment **D**; (iii) Z-L-Iva-L-Leu-(Aib)₃-OrBu; and (iv) Z-L-Ile-L-Iva-L-Leu-(Aib)₃-OrBu, the C-terminal penta- and hexapeptides of segment **B**. The

molecular structures of the last three peptides are illustrated in Figures 3-5. Their backbone torsion angles are listed in Table 1.

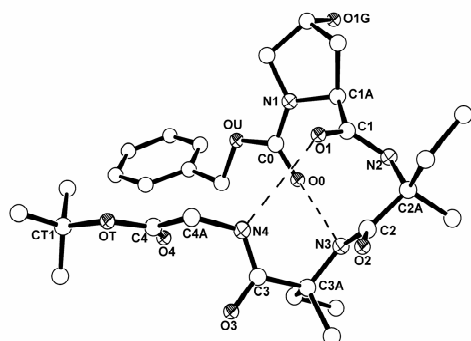


Figure 3. X-ray diffraction structure of Z-L-Hyp-L-Iva-D-Iva-Gly-OrBu with atom numbering. H-atoms were omitted for clarity. Dashed lines represent intramolecular H-bonds.

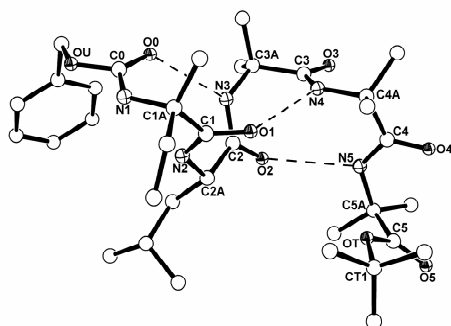


Figure 4. X-ray diffraction structure of Z-L-Iva-L-Leu-(Aib)₃-OrBu with atom numbering. Only the major occupancy site of the L-Iva C^γ atom is shown. H-atoms were omitted for clarity. Dashed lines represent intramolecular C=O ... H-N H-bonds.

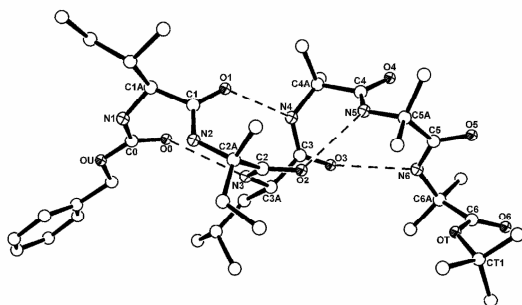


Figure 5. X-ray diffraction structure of Z-L-Ile-L-Iva-L-Leu-(Aib)₃-OrBu acetonitrile hemisolvate with atom numbering. H-atoms were omitted for clarity. Dashed lines represent intramolecular C=O ... H-N H-bonds.

Table 1. Backbone torsion angles [°] for the peptides studied in this work

Torsion angle	Z-L-Hyp-L-Iva-D-Iva-Gly-OrBu	Z-L-Iva-L-Leu-(Aib) ₃ -OrBu	Z-L-Ile-L-Iva-L-Leu-(Aib) ₃ -OrBu
ω_0	-170.2(4)	-177.6(8)	-165.6(8)
ϕ_1	-56.4(5)	-58.4(11)	-62.3(11)
ψ_1	132.5(4)	-23.3(11)	-48.0(11)
ω_1	173.0(3)	178.0(8)	-173.1(7)
ϕ_2	55.3(5)	-64.6(10)	-56.2(11)
ψ_2	39.2(5)	-10.9(11)	-30.8(12)
ω_2	169.4(4)	173.2(8)	-175.3(8)
ϕ_3	72.8(6)	-54.9(10)	-58.8(11)
ψ_3	28.2(7)	-33.8(10)	-28.1(12)
ω_3	171.2(5)	-176.1(7)	179.3(8)
ϕ_4	-79.3(8)	-73.5(10)	-53.4(11)
ψ_4	171.6(5) ^[a]	-7.4(10)	-33.5(10)
ω_4	178.0(5) ^[b]	-167.7(8)	-173.8(7)
ϕ_5		50.9(11)	-59.1(11)
ψ_5		43.3(12) ^[c]	-37.8(12)
ω_5		174.8(10) ^[d]	-164.1(9)
ϕ_6			46.4(13)
ψ_6			48.5(11) ^[e]
ω_6			171.1(10) ^[f]

[a] N4-C4A-C4-OT. [b] C4A-C4-OT-CT1. [c] N5-C5A-C5-OT. [d] C5A-C5-OT-CT1. [e] N6-C6A-C6-OT. [f] C6A-C6-OT-CT1.

In the structure of the tetrapeptide (Figure 3), two C=O ... H-N intramolecular H-bonds are seen between the peptide N3-H and urethane C0=O groups and between the peptide N4-H and peptide C1=O1 groups. Both H-bonds are weak^[12] (Table S1 in *Supporting Information*). The N-terminal -L-Hyp-L-Iva- β -turn structure^[13] is non-helical type-II, while the next one (-L-Iva-D-Iva-) is helical type-III'. Both Iva residues, independent of their configuration, adopt ϕ, ψ torsion angles falling in the left-handed helical region of the Ramachandran map. Two intermolecular H-bonds involve the peptide N2-H and side-chain Hyp O-H groups as donors, and the peptide C2=O2 and C1=O1 as acceptors, respectively. The -D-Iva-L-Iva- sequence in the tripeptide Z-D-Iva-L-Iva-Gly-OrBu, shorter by one residue at the N-terminus, is also helical.^[11] The structure of the strictly related tetrapeptide Z-L-Pro-L-Iva-D-Iva-Gly-OrBu also shows a non-helical conformation with two consecutive β -turns of type II - III'.^[11] These findings are in line with the well-known structural bias of the L-Pro / L-Hyp residues for a *semi*-extended [or poly-(Pro)_n II] conformation^[14] and of the Iva helical screw-sense indifference, due to the small difference in length between its two side chains.^[15]

The pentapeptide molecule (Figure 4), particularly rich in helicogenic Aib residues,^[16] is highly folded. The -L-Iva-L-Leu-Aib-Aib- segment is stabilized by three consecutive C=O ... H-N intramolecular H-bonds (C0=O0 ... H-N3, C1=O1 ... H-N4, C2=O2 ... H-N5), generating a full turn of a 3_{10} -helix.^[17] However, this right-handed structure is not regular, in particular at the level of the L-Leu² and Aib⁴ residues, where the corresponding ψ torsion angles are well below the typical -30° value, generating type-I instead of type-III β -turns. Nonetheless, the intramolecular H-bonds exhibit normal N ... O distances and N-H ... O angles. The typical screw-

sense inversion with respect to the preceding residues in the backbone, usually observed at the C-terminus of a 3_{10} -helical peptide for a C^α -tetrasubstituted α -amino acid ester,^[16] is noted also in this compound. The pentapeptide molecules are held together head-to-tail through a C4=O4 ... H-N1 intermolecular H-bond.

At partial variance with its pentapeptide synthetic precursor, the hexapeptide (Figure 5) adopts a regular, right-handed, 3_{10} -helical structure in the crystalline state (Table 1). Four consecutive, type-III β -turns are seen, each stabilized by a C=O ... H-N intramolecular H-bond. The H-bonds involve the N3-H, N4-H, N5-H and N6-H groups as donors and the C0=O0, C1=O1, C2=O2 and C3=O3 groups as acceptors, respectively. Only the N-terminal H-bond is rather weak. Also in this compound, we observe a screw-sense inversion for the C-terminal, helical Aib residue. Two intermolecular H-bonds (C4=O4 ... H-N1 and C5=O5 ... H-N2), the latter quite weak, stabilize the head-to-tail packing mode of the helical molecules in the crystal.

From this crystal-state conformational analysis, it seems reasonable to conclude that most of the N-terminal heptapeptide segment **B** of integramide A possesses a strong propensity for a regular, right-handed, 3_{10} -helical structure. On the other hand, the C-terminal segment **D** is not helical *per se*, most probably because of the presence of a Janus-headed Hyp residue located at position 1. However, it would not be surprising to see this segment as well in a regular folded conformation when incorporated at the C-terminus of a pre-existing helical stretch.

Solution Conformational Analysis. We investigated the conformational preferences in solution for the two hexadecapeptide diastereomers, L-Iva¹⁴-D-Iva¹⁵ and D-Iva¹⁴-L-Iva¹⁵, and for natural integramide A under different solvent and temperature conditions by use of CD, FT-IR absorption and 2D-NMR techniques.

The CD spectra of the two synthetic compounds in MeOH (methanol), TFE, and 100 mM sodium dodecylsulfate (SDS) aqueous solutions are shown in Figure 6. In Figure 7, the two curves in TFE are compared with that of natural integramide A in the same fluoroalcohol. By changing solvent, no dramatic alterations are seen in the CD patterns, highlighting the remarkable secondary structure stability of the two compounds. This conclusion is corroborated by the absence of any variation in the spectra by heating from 5 to 55 °C in MeOH solution (not shown). The shape of the CD patterns clearly indicate that both compounds fold in a right-handed helical structure of the mixed 3_{10} -/ α -type [in MeOH, the 3_{10} -helix seems to prevail, whereas in SDS the α -helix tends to be more populated]. This information was extracted from the occurrence of two negative maxima near 205 and 225 nm and one positive maximum at about 195 nm, and from the ellipticity ratio $[\Theta]_R^{225}/[\Theta]_R^{205}$, known to be <0.50 for a high population of 3_{10} -helix and >0.60 for a high population of α -helix.^[18] In general, the highest ellipticity and, as a consequence, the most significant structural percentage is seen in the helix-supporting solvent TFE^[19] for both compounds. The CD patterns of the two hexadecapeptide diastereomers are similar to each other and to that of natural integramide A, suggesting that the chirality inversion in the -Iva¹⁴-Iva¹⁵ dipeptide segment does not induce any significant change in the overall peptide secondary structure. However, only the CD curve of the L-Iva¹⁴-D-Iva¹⁵ peptide matches almost perfectly that of natural integramide A. Finally, the CD curves of the Z/OtBu protected pentadecapeptides and of the Ac/OtBu protected hexadecapeptide synthetic precursors (not shown) nearly overlap those of the two final diastereomeric compounds, showing that the observed 3_{10} -/ α -helical conformation is already attained at the 15-mer level and also before removal of the OtBu C-terminal protecting group.

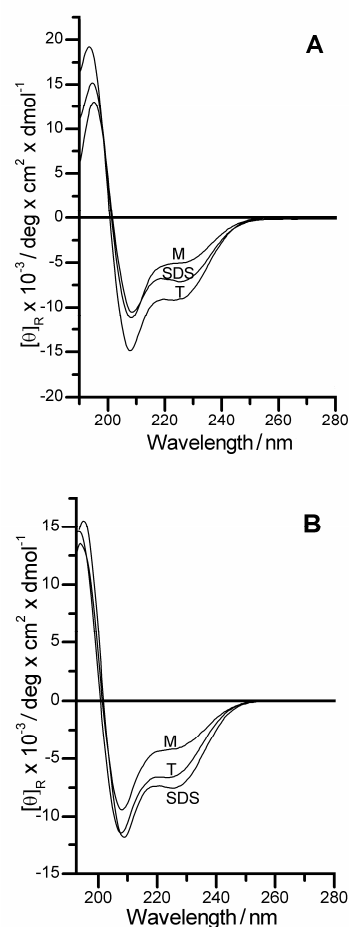


Figure 6. CD spectra for the two synthetic hexadecapeptide diastereomers L-Iva¹⁴-D-Iva¹⁵ (A) and D-Iva¹⁴-L-Iva¹⁵ (B) in MeOH (M), TFE (T), and 100 mM SDS aqueous solutions. Peptide concentration: 1 mM.

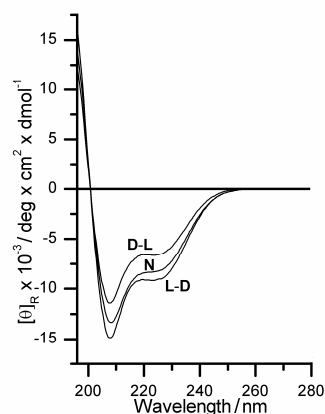


Figure 7. CD spectra for the two synthetic hexadecapeptide diastereomers L-Iva¹⁴-D-Iva¹⁵ (L-D) and D-Iva¹⁴-L-Iva¹⁵ (D-L), and natural integramide A (N) in TFE solution. Peptide concentration: 1 mM.

The FT-IR absorption spectra in the conformationally informative N-H stretching region for the short, Z/OtBu protected

segments **B**, **C** and **D** (the latter for the L-Iva¹⁴-D-Iva¹⁵ diastereomer) in CDCl₃ solution at two concentrations are reported in Figure 8. The curves change only slightly from 1.0 to 0.1 mM concentration (except for segment **C**, but only below 3320 cm⁻¹). This finding suggests that almost all observed C=O ... H-N H-bonding is intramolecular. The ratio between the areas of the 3350 cm⁻¹ band (associated with H-bonded NH groups^[20]) and the band(s) above 3400 cm⁻¹ (associated with free, solvated NH groups) is much lower for segment **C**, indicating that the latter peptide exhibits a remarkably reduced tendency to fold, probably related not only to its short main-chain length, but to its specific sequence as well, as it lacks any heliogenic C^α-methylated α-amino acid in the N-terminal doublet. This structural information agrees with that found from the X-ray diffraction analysis described above. Consistent with this result, in the two longer segments **C-D** and **B-C-D** (spectra not shown), and in the two Ac/OtBu-protected hexadecapeptide diastereomers (Figure 8), all containing the **C** segment, we find that the band at 3350 cm⁻¹ is significantly broadened, implying some conformational heterogeneity in this part of the molecule. Furthermore: (i) Since the spectra of the two hexadecapeptide diastereomers are very similar, this spectroscopic technique does not allow any specific assignment. (ii) In these two spectra, the extremely weak band above 3400 cm⁻¹ is indicative of the occurrence of highly folded species. (iii) At concentrations above 1.0 mM, the curves of all Z-protected synthetic intermediates do not suggest the onset of any significant amount of self-aggregated species, in contrast with those of the two Ac-blocked hexadecapeptide diastereomers which are strongly indicative of self-aggregation (spectra not shown). (iv) Unfortunately, we could not record the spectra of the two final, synthetic Ac/OH hexadecapeptides due to their very low solubilities in CDCl₃.

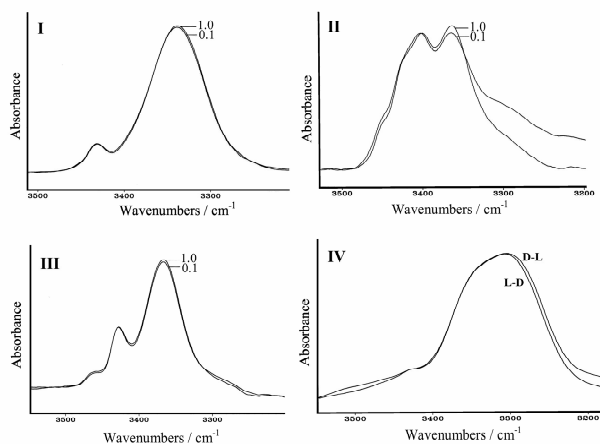


Figure 8. FT-IR absorption spectra (N-H stretching region) of the Z/OtBu protected segments **B** (I), **C** (II), and L-Iva-D-Iva diastereomer of **D** (III) at the concentrations 1 mM (1.0) and 0.1 mM (0.1). Panel IV shows the corresponding spectra for the two synthetic, Ac/OtBu protected hexadecapeptide diastereomers L-Iva¹⁴-D-Iva¹⁵ (**L-D**) and D-Iva¹⁴-L-Iva¹⁵ (**D-L**) at 1 mM concentration. Solvent: CDCl₃.

A more detailed conformational characterization of integramide A was carried out by 2D-NMR spectroscopy. This study was performed in TFE-*d*₂ solution where the peptide exhibits a high propensity to fold into a helical structure as indicated by CD. The spin systems of the Gly, Leu, Hyp and Ile residues were identified using DQF-COSY and TOCSY spectra, while HMQC and HMBC experiments were used for the Aib and Iva residues. The sequential

assignment was performed using NOESY spectra. Relevant regions of the NOESY spectrum at $\tau_m = 250$ ms are shown in Figures 9 and 10. The proton chemical shift assignment is reported in Table S2 (*Supporting Information*). A summary of the NOE connectivities is shown in Figure 11.

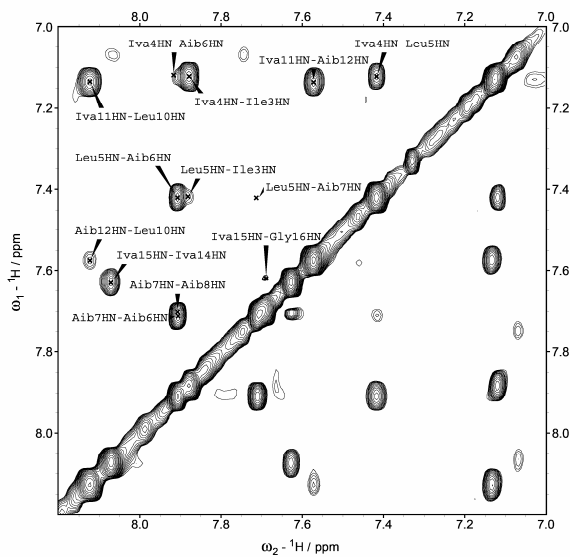


Figure 9. Amide region of the NOESY spectrum (600 MHz, $\tau_m = 250$ ms) of integramide A (1.45 mM in TFE, *d*₂; 300 K). Medium-range (*i* → *i*+2) interactions are marked.

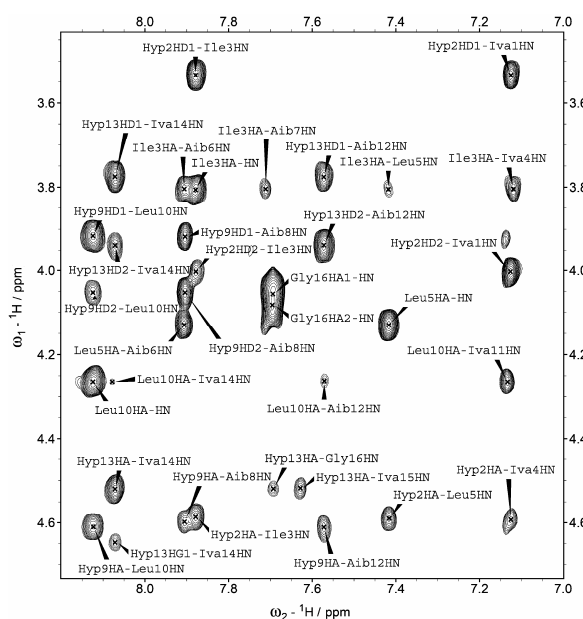


Figure 10. Fingerprint region of the NOESY spectrum (600 MHz, $\tau_m = 250$ ms) of integramide A (1.45 mM in TFE, *d*₂; 300 K). Medium-range (*i* → *i*+2, *i* → *i*+3, and *i* → *i*+4) interactions are marked.

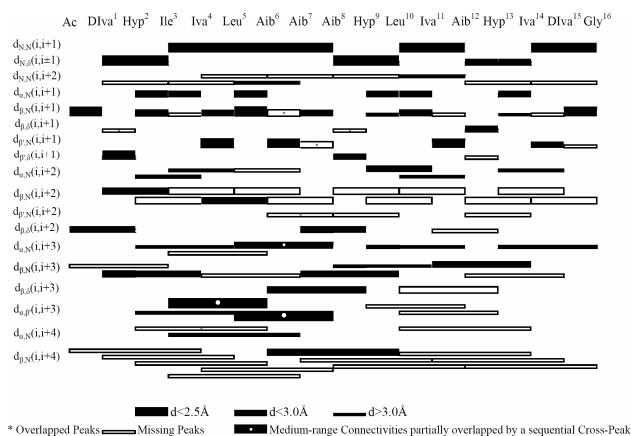


Figure 11. Summary of the NOESY connectivities for integramide A (1.45 mM in TFE, d_2 ; 300 K). Peaks are grouped into three classes based upon their integrated volumes.

Despite the presence of three Hyp residues, no trace of *cis* configuration at the Xxx-Hyp bonds was detected. The 1D spectrum does not show minor peaks, and no sequential $C^{\alpha}H-C^{\alpha}H$ NOESY cross-peaks were found. All NH-NH sequential connectivities are present, as well as some NH(*i*)-NH(*i*+2) connectivities. These results are consistent with a helical structure, which is not interrupted by the Hyp residues, as also confirmed by the presence in the NOESY spectrum of all of the connectivities between the Hyp $C^{\beta}H$ protons and the NH proton of both the preceding and the following residues. A number of $C^{\alpha}H(i)$ -NH(*i*+3) cross peaks, together with $C^{\alpha}H(i)$ -NH(*i*+2) and $C^{\alpha}H(i)$ -NH(*i*+4) cross peaks, were observed. Together, these data support the presence of a mixed 3_{10} -/ α -helical conformation.

The two methyl groups in the Aib residues belonging to chiral peptides are diastereotopic. Consequently, the carbon atoms of the two methyl groups (labeled as β and β') are expected to resonate at two different chemical shifts, above and below 25 ppm (Figure S1, *Supporting Information*). Jung *et al.*^[21] have shown that the presence of a chiral center adjacent to two *gem*-methyl groups, as in an Aib residue, induces a chemical shift difference between these pro-chiral methyl carbons, but not higher than 0.5 ppm. However, if the observed difference in the ^{13}C chemical shifts (termed chemical non-equivalence, CNE) of the two pro-chiral methyl carbons is 2 ppm or higher, this indicates the presence of a stable helical conformation. In Table S3 (*Supporting Information*) the CNE values for the four Aib residues of integramide A are reported. All values are higher than 2 ppm, confirming the occurrence of a helical structure in TFE solution. The stereospecific assignment of the two diastereotopic methyl groups was achieved through the C_{β} -selective HMQC spectrum, using the method reported by Bellanda *et al.*^[22]

The conformational properties of integramide A were further investigated by distance geometry and restrained molecular dynamics (MD) calculations. A total of 99 inter-proton distance restraints were derived from the NOESY spectrum (Table 2) and used in the SA protocol. Out of the 150 structures that were generated, 100 had violations of the NOE restraints lower than 0.5 Å. The 33 structures with a total energy < 300 kcal/mol were selected. Their superposition is shown in Figure 12. All of these structures converge to a well-defined, mixed 3_{10} -/ α -helical conformation throughout the sequence, with a backbone average pair-wise root-mean-square deviation of 0.26 ± 0.10 Å (Table 3). The lowest-energy 3D-structure, shown in Figure 13, exhibits a clear

amphipathic character with the three L-Hyp residues at positions 2, 9, and 13 forming the hydrophilic face.

Table 2. NOE constraints, deviations from idealized geometry, and mean energies for the NMR-based structure of integramide A

Number of NOEs	
total	99
intraresidue	32
sequential	46
<i>i,i+n</i> , <i>n</i> =2, 3, 4	21
Mean rmsd ^[a] from ideality of accepted structures	
bonds [Å]	0.0097
angles [°]	1.13
improper [°]	37.40
NOEs [Å]	0.19
Mean energies [kcal/mol] of accepted structures	
E _{overall}	299.1
E _{bond}	23.7
E _{angle}	90.9
E _{NOE}	165.7

[a] Root-mean-square deviation.

Table 3. Average values [°] of torsion angles ϕ_m and ψ_m and the relative standard deviations resulting from the 33 calculated structures (energy < 300 kcal/mol) of integramide A

Residue	ϕ_m	$\Delta\phi$	ψ_m	$\Delta\psi$
D-Iva ¹	-		-42.6	±0.5
L-Hyp ²	-84.0	±1.1	3.3	±1.6
L-Ile ³	-80	±2	-21.4	±1.7
L-Iva ⁴	-73.3	±0.9	-27.1	±0.6
L-Leu ⁵	-81.5	±1.4	-25.4	±0.8
Aib ⁶	-88.3	±0.9	-43.0	±0.7
Aib ⁷	-73.5	±0.6	-23.4	±1.4
Aib ⁸	-68.3	±1.7	-61.5	±1.1
L-Hyp ⁹	-70.6	±0.6	-27	±3
L-Leu ¹⁰	-72.7	±1.9	-29.6	±1.5
L-Iva ¹¹	-82	±3	-40.4	±1.0
Aib ¹²	-34.2	±1.3	-53.1	±0.7
L-Hyp ¹³	-72.8	±0.6	-44.3	±1.7
L-Iva ¹⁴	-50.4	±0.8	-22.1	±0.6
D-Iva ¹⁵	-84.1	±2.8	-78.7	±0.7
Gly ¹⁶	-29.6	±1.5	-	

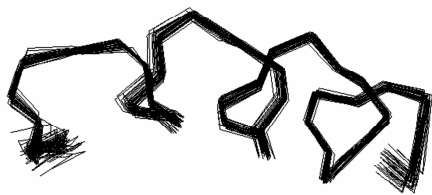


Figure 12. Backbone representation of the 33 structures with energy < 300 kcal/mole resulting from the MD calculations of integramide A with the backbone atoms superimposed.

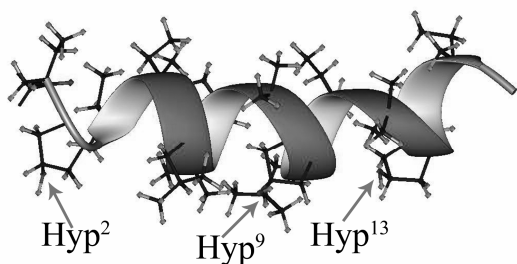


Figure 13. Representation of the 3D-structure with the lowest energy obtained for integramide A. The three L-Hyp residues are labeled.

Conclusions

Our interest for the study of integramides not only originated from their intrinsic activity as effective inhibitors of HIV-1 integrase,^[4] but also from the observation that their primary structures are closely related to those of peptaibols^[23] / peptaibiotics,^[7c,24] a class of naturally-occurring peptides characterized by a high occurrence of the strongly 3_{10} / α -helicogenic, C ^{α} -methylated α -amino acids Aib^[16] and Iva^[15].

Although synthetic methods for peptides based on sterically demanding C ^{α} -methylated α -amino acids have been already described,^[7] the total syntheses of integramide A, a 16-amino acid long peptide, and its D-Iva¹⁴-L-Iva¹⁵ diastereomer are notable achievements. Indeed, these compounds present some remarkable challenges due to the sterically hindered nature of multiple amino acids, the acid sensitivity of three tertiary amide bonds, and the propensity to cyclize of a few N-terminal dipeptides with the related potential loss of two residues from their sequence.

Our present, very detailed, 3D-structural analysis on integramide A and selected short sequences clearly supports the view that the peptide inhibitor has a predominantly 3_{10} / α -helical structure with amphipathic features under the variety of the experimental conditions used. Noteworthy, in the C-terminal half of the molecule the Aib(Iva) backbone constraints outweigh the Hyp conformational preference for the *semi*-extended type-II poly-(L-Pro)_n conformation. This conclusion agrees well with literature reports on model

peptides and on naturally occurring peptaibiotics with repeating Aib(Iva)-L-Pro(Hyp) sequences as well.^[25] These compounds are characterized by a β -turn ribbon structure in which the regularity of the 3_{10} -helical backbone ϕ, ψ torsion angles is preserved despite a heavy presence of Pro(Hyp) residues, which is more than compensated for by the extremely strong folding propensity of the preceding Aib(Iva) residues. Remarkably, in a β -turn ribbon segment the orientation of the peptide carbonyls with respect to the helix axis is not significantly modified as compared to that of these same groups in the 3_{10} -helix, but some of them cannot form H-bonds with the N-alkylated Pro(Hyp) residues. As a result, these C=O groups are available to interact with H-bonding donor solvents or with other surrounding peptide (protein) molecules.

A variety of approaches has been used to identify peptides that inhibit HIV-1 integrase.^[3] Of particular significance are the conclusions of Roques and coworkers^[3c] who isolated a 12-mer peptide inhibitor (EBR28) that binds tightly to the enzyme. NMR structure analysis showed that under favorable experimental conditions this peptide adopts an α -helical conformation with amphipathic properties. The authors' evidence further suggest that the peptide binds the integrase catalytic core, thus impairing the enzyme dimerization motif essential for its activity. Moreover, the hydrophobic face of the α -helix seems implicated in this interaction. We believe that the 16-mer peptide main-chain length, the stable helical properties, and the strongly amphipathic nature of integramides might mimic the corresponding characteristics of EBR28 and its proposed mechanism of integrase inhibition. It is also our view that X-ray diffraction analyses of peptide inhibitor – integrase complexes can be extremely useful to elucidate this mechanism and optimize drug candidates that target integration of HIV. In this connection, the low conformational flexibility shown by integramide A, typical of the highly crystalline Aib/Iva-rich peptides,^[15,16] will facilitate such analyses.

Experimental Section

Synthesis and Characterization of Peptides. The strategy of synthesis of the peptides discussed in this work is illustrated in *Scheme 1*. Details of their characterization are reported in the *Supporting Information*.

X-ray Diffraction. Single crystals of Z-L-Hyp-L-Iva-D-Iva-Gly-*Or*Bu and Z-L-Iva-L-Leu-(Aib)₃-*Or*Bu were grown from ethyl acetate / petroleum ether, while those of Z-L-Ile-L-Iva-L-Leu-(Aib)₃-*Or*Bu by slow evaporation from acetonitrile. Diffraction data were collected at T = 293(2) K with CuK α radiation ($\lambda = 1.54178$ Å) using a Philips PW 1100 diffractometer in the $\theta - 2\theta$ scan mode up to $\theta = 60^\circ$. The structures were solved by direct methods with the SIR 2002 program.^[26a] Refinements were carried out by least-squares procedures on F^2 , using all data, by application of the SHELXL 97 program.^[26b] All non-H atoms were refined anisotropically. H-atoms were calculated at idealized positions and refined using a riding model.

Z-L-Hyp-L-Iva-D-Iva-Gly-OrBu. Formula: C₂₉H₄₄N₄O₈; formula weight: 576.7; orthorhombic, space group P2₁2₁2₁; unit cell parameters: $a = 9.440(2)$, $b = 11.768(2)$, $c = 29.962(4)$ Å; $V = 3328.5(10)$ Å³; $Z = 4$; $D_{\text{calcd}} = 1.151$ Mg m⁻³; crystal size: $0.40 \times 0.15 \times 0.07$ mm³; data / parameters: 3369 / 359; $R_1 = 0.059$ [on $F \geq 4\sigma(F)$]; $wR_2 = 0.176$ (on F^2 , all data); goodness of fit on F^2 : 0.951; largest peak and hole in the final difference Fourier map: 0.264 and -0.188 e Å⁻³.

Z-L-Iva-L-Leu-(Aib)₃-OrBu. Formula: C₃₅H₅₇N₅O₈; formula weight: 675.9; monoclinic, space group P2₁; unit cell parameters: $a = 10.096(2)$, $b = 17.798(3)$, $c = 11.554(2)$ Å, $\beta = 105.28(5)^\circ$; $V = 2002.7(6)$ Å³; $Z = 2$; $D_{\text{calcd}} = 1.121$ Mg m⁻³; crystal size: $0.45 \times 0.40 \times 0.10$ mm³; data / restraints / parameters: 3279 / 42 / 430; $R_1 = 0.141$ [on $F \geq 4\sigma(F)$]; $wR_2 = 0.334$ (on F^2 , all data); goodness of fit on F^2 : 1.696; largest peak and hole in the final difference Fourier map: 0.530 and -0.630 e Å⁻³. The C ^{γ} atom of the L-Iva residue is disordered and was refined on two sites with population parameters 0.55 and 0.45, respectively.

Z-L-Ile-L-Iva-L-Leu-(Aib)₃-OrBu acetonitrile emisolvate. Formula: C₄₁H₆₈N₆O₉ \times $\frac{1}{2}$ CH₃CN; formula weight: 809.5; orthorhombic, space group C222₁; unit cell parameters: $a = 13.580(2)$, $b = 19.486(3)$, $c = 38.283(4)$ Å; $V = 10130(2)$ Å³; $Z = 8$; $D_{\text{calcd}} = 1.062$ Mg m⁻³; crystal size: $0.30 \times 0.20 \times 0.07$ mm³; data / restraints / parameters: 4130 / 44 / 519; $R_1 = 0.082$ [on $F \geq 4\sigma(F)$]; $wR_2 = 0.233$ (on F^2 , all data); goodness of fit on F^2 :

0.926; largest peak and hole in the final difference Fourier map: 0.332 and -0.264 e^{-3} . The co-crystallized acetonitrile molecule occupies a $(\frac{1}{2}, y, \frac{1}{4})$ special position and shows orientational disorder. CCDC-726112–726114 contain the supplementary crystallographic data for this paper. These data can be obtained from The Cambridge Crystallographic Data Centre via www.ccdc.cam.ac.uk/data_request/cif.

Circular Dichroism. The CD spectra were obtained on a Jasco (Tokyo, Japan) J-715 spectropolarimeter. Cylindrical fused quartz cells (Hellma) of 0.1 mm path length were used. The values are expressed in terms of $[\Theta]_R$, residue molar ellipticity ($\text{deg} \cdot \text{cm}^2 \cdot \text{dmol}^{-1}$). Spectrograde MeOH and TFE (Acros, Geel, Belgium) were used as solvents.

Infrared Absorption. The FT-IR absorption spectra were recorded using a Perkin-Elmer model 1720 X FT-IR spectrophotometer, nitrogen flushed, equipped with a sample-shuttle device, at 2 cm^{-1} nominal resolution, averaging 100 scans. Cells with path lengths of 0.1, 1.0, and 10 mm (with CaF_2 windows) were used. Spectrograde deuteriochloroform (99.8 % *d*) was purchased from Aldrich (St. Louis, MO). Solvent (baseline) spectra were recorded under the same conditions.

Chiral Liquid Chromatography.^[10] Total hydrolysis: 0.48 mg of the synthetic L-Iva¹⁴-D-Iva¹⁵ hexadecapeptide or its D-Iva¹⁴-L-Iva¹⁵ diastereomer were hydrolyzed in 0.5 mL of a 6 M HCl solution for 18 h at 120 °C and evaporated to dryness. Derivatization: 1 M NaHCO_3 (100 μL) and the Marfey's reagent, N^{α} -(2,4-dinitro-5-fluorophenyl)-L-alanine amide, FDNP-L-Ala-NH₂ (Sigma, St. Louis, MO) (1% in acetone, 100 μL) were added. The mixture was sonicated and incubated at 40 °C for 1 h in a closed vial. 1 M HCl (100 μL) and dimethylsulfoxide (200 μL) were added, and aliquots of 5 μL injected into the HPLC column. Instruments: an HP model 1100 apparatus with a quaternary pump (Hewlett-Packard, Waldbronn, Germany) and a photo-diode array detector set at 340 nm; LiChroCART Superspher 60 RP-Select B column (250 mm \times 4 mm ID; 4 μm particle size; Merck, Darmstadt, Germany). Gradient elution: eluant A: 50 mM triethylammonium phosphate buffer, pH 3.0; eluant B: acetonitrile (100%); gradient: 15% B to 60% B in 75 min; flow rate: 1.2 mL/min.

Chiral Gas Chromatography. Total hydrolysis: 0.1 mg of natural integramide A^[4] or the synthetic L-Iva¹⁴-D-Iva¹⁵ hexadecapeptide were hydrolyzed in 0.5 mL of a 6 M HCl solution for 18 h at 120 °C and evaporated to dryness. Then, HCl in 2-propanol (0.5 mL; generated from a mixture of AcCl / 2-propanol 2:8 v/v) was added and the esterification was performed for 1 h at 100 °C in a closed vial. Solvents were removed in a stream of nitrogen, CH_2Cl_2 (250 μL) and trifluoroacetic anhydride (50 μL) were added, and the mixture heated at 100 °C for 20 min. Solvents were removed in a stream of nitrogen, CH_2Cl_2 (200 μL) was added, and 5 μL aliquots were injected into the gas chromatographic (GC) column. Instruments: a GC-MS (mass spectrometry) apparatus, with an A17 GC and a Shimadzu 5000 MS, was used. For chiral analysis of amino acid derivatives, a Chirasil-L-Val capillary column (25 m \times 0.35 mm ID; Varian, Darmstadt, Germany) and helium as carrier gas were employed. Solvents and reagents were from Merck.

Mass Spectrometry.^[10b] For ESI-CID-MS measurements, a calibrated LCQ-MSTM (Thermo Quest, Finnigan MAT, San José, CA) was used. N_2 served as sheath gas and auxiliary gas. He (purity >99.9990 %, Messer-Griesheim, Krefeld, Germany) was used as collision gas. The temperature of the heated capillary was 250 °C. Sheath gas and auxiliary gas were set at 40 and 10 relative units, respectively. Ion source CID-MS was performed at 0 and 45% relative collision energies. Sequence analyses were carried out in the positive ionization mode. The *m/z* values were recorded in the centroid mode and have an accuracy of ± 0.5 Da.

Nuclear Magnetic Resonance. NMR experiments were carried out on a Bruker AVANCE DMX-600 spectrometer. The peptide concentration was 1.45 mM in deuterated (*d*₂) TFE. The alcohol -OH signal was suppressed by presaturation during the relaxation delay. All homonuclear spectra were acquired by collecting 512 experiments, each one consisting of 64 scans and 2K data points. The spin systems of protein amino acid residues were identified using standard DQF-COSY^[27] and CLEAN-TOCSY^[28] spectra. In the latter case, the spin-lock pulse sequence was 70 ms long. The assignment of methyl groups belonging to the same Aib residue was obtained by means of 2D ¹H-¹³C correlation spectra. To optimize the digital resolution in the carbon dimension, HMQC and HMBC spectra were acquired using selective excitation by means of Gaussian-shaped pulses with 1% truncation.^[29] The C β -selective HMQC spectra with gradient coherence selection^[30] were recorded with 224 t₁ increments of 270 scans and 2K points each.^[31] A spectral width of 16 ppm centered at 22 ppm in F1 was used, yielding a digital resolution of 2.36 Hz/pt prior to zero filling. HMBC experiments^[32] with selective excitation in the CO region were performed using a long-range coupling constant of 7.5 Hz, a spectral width in F1 of 15 ppm centered at 176 ppm, 250 t₁ experiments of 800 scans, and 4K points in F2. The digital resolution in F1, prior to zero filling, was 2.2 Hz/pt. NOESY experiments were used for sequence specific assignment. To avoid the problem of spin diffusion, the build-up curve of the volumes of NOE cross-peaks as a function of mixing time (50 to 500 ms) was determined first (data not shown). The mixing time of the NOESY experiments used for inter-proton distance determination ranged from 200 to 250 ms,

that is, in the linear part of the NOE build-up curve. Inter-proton distances were obtained by integration of the NOESY spectra using the XEASY^[33] package. The calibration was based on the average of the integration values of the cross peaks due to the interactions between the two β -geminal protons of the Leu side-chain residues and the two δ -geminal protons of the Hyp side-chain residues, set to a distance of 1.8 Å. When peaks could not be integrated because of partial overlap, a distance corresponding to the maximum limit of detection of the experiment (4.0 Å) was assigned to the corresponding proton pair.

Distance geometry and MD calculations were carried out using the simulated annealing (SA) protocol of the XPLOR-NIH 2.9.6 program.^[34] For distances involving equivalent or non-stereo-assigned protons, r^6 averaging was used. The MD calculations involved a minimization stage of 100 cycles, followed by SA and refinement stages. The SA consisted of 30 ps of dynamics at 1500 K (10000 cycles, in 3 fs steps) and of 30 ps of cooling from 1500 to 100 K in 50 K decrements (15000 cycles, in 2 fs steps). The SA procedure, in which the weights of NOE and nonbonded terms were gradually increased, was followed by 200 cycles of energy minimization. In the SA refinement stage, the system was cooled from 1000 to 100 K in 50 K decrements (20000 cycles, in 1 fs steps). Finally, the calculations were completed with 200 cycles of energy minimization using a NOE force constant of 50 kcal/mol. The generated structures were visualized using the MOLMOL^[35] (version 2K.2) program.

- [1] Y. Goldgur, R. Craigie, G. H. Cohen, T. Fujiwara, T. Yoshinaga, T. Fujishita, H. Sugimoto, T. Endo, H. Murai, D. R. Davies, *Proc. Natl. Acad. Sci. USA* **1999**, *96*, 13040-13043.
- [2] a) R. Craigie, *J. Biol. Chem.* **2001**, *276*, 23213-23216; b) S. P. Singh, F. Pelaez, D. J. Hazuda, R. B. Lingham, *Drugs Future* **2005**, *30*, 277-299; c) R. Dayam, R. Gundla, L. Q. Al-Mawsawi, N. Neamati, *Med. Res. Rev.* **2008**, *28*, 118-154; d) T. A. Prikazchikova, A. M. Sychova, Yu. Yu. Agapkina, D. A. Alexandrov, M. B. Gottikh, *Russian Chem. Rev.* **2008**, *77*, 421-434.
- [3] a) R. A. Puras Lutzke, N. A. Leppens, P. A. Weber, R. A. Houghten, R. H. A. Plasterk, *Proc. Natl. Acad. Sci. USA* **1995**, *92*, 11456-11460; b) R. G. Maroun, D. Krebs, M. Rashani, H. Porumb, C. Auclair, F. Troalen, S. Fermandjian, *Eur. J. Biochem.* **1999**, *260*, 145-155; c) V. R. de Soultrait, A. Caumont, V. Parissi, N. Morellet, M. Ventura, C. Lenoir, S. Litvak, M. Fournier, B. Roques, *J. Mol. Biol.* **2002**, *318*, 45-48; d) L. Zhao, M. K. O'Reilly, M. D. Shultz, J. Chmielewski, *Bioorg. Med. Chem. Lett.* **2003**, *13*, 1175-1177; e) K. Krajewski, C. Marchand, Y.-Q. Long, Y. Pommier, P. P. Roller, *Bioorg. Med. Chem. Lett.* **2004**, *14*, 5595-5598; f) I. O. Gleenberg, O. Avidan, Y. Goldgur, A. Hershorn, A. Hizi, *J. Biol. Chem.* **2005**, *280*, 21987-21996; g) H.-Y. Li, Z. Zawahir, L. D. Song, Y.-Q. Long, N. Neamati, *J. Med. Chem.* **2006**, *49*, 4477-4486; h) P. Cherepanov, A. L. B. Ambrosio, S. Rahman, T. Ellenberger, A. Engelman, *Proc. Natl. Acad. Sci. USA* **2005**, *102*, 17308-17313; i) A. Armon-Omer, A. Levin, Z. Hayouka, K. Butz, F. Hoppe-Seyley, S. Loya, A. Hizi, A. Friedler, A. Loyter, *J. Mol. Biol.* **2008**, *376*, 971-982.
- [4] S. B. Singh, K. Herath, Z. Guan, D. L. Zink, A. W. Dombrowski, J. D. Polishook, K. C. Silverman, R. B. Lingham, P. J. Felock, D. J. Hazuda, *Org. Lett.* **2002**, *4*, 1431-1434.
- [5] M. De Zotti, F. Formaggio, B. Kaptein, Q. B. Broxterman, P. J. Felock, D. J. Hazuda, S. B. Singh, H. Brückner, C. Toniolo, *ChemBioChem* **2009**, *10*, 87-90.
- [6] T. Sonke, B. Kaptein, W. H. J. Boesten, Q. B. Broxterman, H. E. Schoemaker, J. Kamphuis, F. Formaggio, C. Toniolo, F. P. J. T. Rutjes, in *Stereoselective Biocatalysis* (Ed: R. N. Patel), Dekker, New York, **1999**, pp. 23-58.
- [7] a) F. Formaggio, Q. B. Broxterman, C. Toniolo, in *Houben-Weyl: Methods of Organic Chemistry, Synthesis of Peptides and Peptidomimetics*, Vol. E22c (Eds: M. Goodman, A. Felix, L. Moroder, C. Toniolo), Thieme, Stuttgart, Germany, **2003**, pp. 292-310; b) H. Brückner, M. Curle, in *Second Forum Peptides* (Eds: A. Aubry, M. Marraud, B. Vitoux), Libbey, London, **1989**, pp. 251-255; c) *Peptidobiotics: Fungal Peptides Containing α -Dialkyl α -Amino Acids*, (Eds: C. Toniolo, H. Brückner), Verlag Helvetica Chimica Acta, Zürich, Switzerland, **2009**.
- [8] L. A. Carpino, *J. Am. Chem. Soc.* **1993**, *115*, 4397-4398.
- [9] A. Moretto, M. Crisma, F. Formaggio, B. Kaptein, Q. B. Broxterman, T. A. Keiderling, C. Toniolo, *Biopolymers (Pept. Sci.)* **2007**, *88*, 233-238.
- [10] a) R. Bhushan, H. Brückner, *Amino Acids* **2004**, *27*, 231-247; b) C. Theis, T. Degenkolb, H. Brückner, *Chem. Biodivers.* **2008**, *5*, 2337-2355.
- [11] M. Crisma, A. Moretto, M. De Zotti, F. Formaggio, B. Kaptein, Q. B. Broxterman, C. Toniolo, *Biopolymers (Pept. Sci.)* **2005**, *80*, 279-293.
- [12] a) C. H. Görbitz, *Acta Crystallogr.* **1989**, *B45*, 390-395; b) C. Ramakrishnan, N. Prasad, *Int. J. Protein Res.* **1971**, *3*, 209-231.
- [13] a) C. M. Venkatachalam, *Biopolymers* **1968**, *6*, 1425-1436; b) G. D. Rose, L. M. Gierasch, J. A. Smith, *Adv. Protein Chem.* **1985**, *37*, 1-109.

- [14] a) E.; Benedetti, A. Bavoso, B. Di Blasio, V. Pavone, C. Pedone, C. Toniolo, G. M. Bonora, *Biopolymers* **1983**, 22, 305-317; b) K. A. Williams, C. M. Deber, *Biochemistry* **1991**, 30, 8919-8923; c) A. Yaron, F. Naider, *Crit. Rev. Biochem. Mol. Biol.* **1993**, 28, 31-81; d) S. J. Eyles, L. M. Gierasch, *J. Mol. Biol.* **2000**, 301, 737-747.
- [15] a) F. Formaggio, M. Crisma, G. M. Bonora, M. Pantano, G. Valle, C. Toniolo, A. Aubry, D. Bayeul, J. Kamphuis, *Pept. Res.* **1995**, 8, 6-15; b) B. Jaun, M. Tanaka, P. Seiler, F. N. M. Kühnle, C. Braun, D. Seebach, *Liebigs Ann. / Rec.* **1997**, 1697-1710; c) G. Valle, M. Crisma, C. Toniolo, R. Beisswenger, A. Rieker, G. Jung, *J. Am. Chem. Soc.* **1989**, 111, 6828-6833; d) R. Bosch, H. Brückner, G. Jung, W. Winter, *Tetrahedron* **1982**, 38, 3579-3583; e) U. Slomczynska, D. D. Beusen, J. Zabrocki, K. Kociolek, A. Redlinski, F. Reusser, W. C. Hutton, M. T. Leplawy, *J. Am. Chem. Soc.* **1992**, 114, 4095-4106.
- [16] a) G. R. Marshall, in *Intra-Science Chemistry Reports*, (Ed: N. Kharasch), Gordon and Breach, New York, **1971**, pp. 305-326; b) I. L. Karle, P. Balarum, *Biochemistry* **1990**, 29, 6747-6756; c) C. Toniolo, M. Crisma, F. Formaggio, C. Peggion, *Biopolymers (Pept. Sci.)* **2001**, 60, 396-419; d) C. Toniolo, *Biopolymers* **1989**, 28, 247-257; e) C. Toniolo, M. Crisma, G. M. Bonora, E. Benedetti, B. Di Blasio, V. Pavone, C. Pedone, A. Santini, *Biopolymers* **1991**, 31, 129-138; f) V. Pavone, B. Di Blasio, A. Santini, E. Benedetti, C. Pedone, C. Toniolo, M. Crisma, *J. Mol. Biol.* **1990**, 214, 633-635.
- [17] a) C. Toniolo, E. Benedetti, *Trends Biochem. Sci.* **1991**, 16, 350-353; b) K. A. Bolin, G. L. Millhauser, *Acc. Chem. Res.* **1999**, 32, 1027-1033.
- [18] a) C. Toniolo, A. Polese, F. Formaggio, M. Crisma, J. Kamphuis, *J. Am. Chem. Soc.* **1996**, 118, 2744-2745; b) F. Formaggio, M. Crisma, P. Rossi, P. Scrimin, B. Kaptein, Q. B. Broxterman, J. Kamphuis, C. Toniolo, *Chem. Eur. J.* **2000**, 6, 4498-4504.
- [19] M. Goodman, A. S. Verdini, C. Toniolo, W. D. Phillips, F. A. Bovey, *Proc. Natl. Acad. Sci. USA* **1969**, 64, 444-450.
- [20] a) E. S. Pysh, C. Toniolo, *J. Am. Chem. Soc.* **1977**, 99, 6211-6219; b) S. C. Yasui, T. A. Keiderling, F. Formaggio, G. M. Bonora, C. Toniolo, *J. Am. Chem. Soc.* **1986**, 108, 4988-4993.
- [21] G. Jung, H. Brückner, R. Bosch, W. Winter, H. Schaal, J. Strähle, *Liebigs Ann. Chem.* **1983**, 1096-1106.
- [22] M. Bellanda, E. Peggion, R. Bürgi, W. van Gunsteren, S. Mammi, *J. Pept. Res.* **2001**, 57, 97-106.
- [23] a) E. Benedetti, A. Bavoso, B. Di Blasio, V. Pavone, C. Pedone, C. Toniolo, G. M. Bonora, *Proc. Natl. Acad. Sci. USA* **1982**, 79, 7951-7954; b) H. Brückner, H. Graf, *Experientia* **1983**, 39, 528-530.
- [24] a) H. Duclouhier, *Chem. Biodivers.* **2007**, 4, 1023-1026; b) B. Leitgeb, A. Szekeres, L. Manczinger, C. Vágvolgyi, L. Kredics, *Chem. Biodivers.* **2007**, 4, 1027-1051; c) T. Degenkolb, J. Kirschbaum, H. Brückner, *Chem. Biodivers.* **2007**, 4, 1052-1067.
- [25] a) I. L. Karle, J. Flippen-Anderson, M. Sukumar, P. Balarum, *Proc. Natl. Acad. Sci. USA* **1987**, 84, 5087-5091; b) B. Di Blasio, V. Pavone, M. Saviano, A. Lombardi, F. Natri, C. Pedone, E. Benedetti, M. Crisma, M. Anzolin, C. Toniolo, *J. Am. Chem. Soc.* **1992**, 114, 6273-6278.
- [26] a) M. C. Burla, M. Camalli, B. Carrozzini, G. L. Cascarano, C. Giacovazzo, G. Polidori, R. Spagna, *J. Appl. Crystallogr.* **2003**, 36, 1103; b) G. M. Sheldrick, *Acta Crystallogr.* **2008**, A64, 112-122.
- [27] M. Rance, O. W. Sørensen, G. Bodenhausen, G. Wagner, R. R. Ernst, K. Wüthrich, *Biochem. Biophys. Res. Commun.* **1983**, 117, 479-485.
- [28] a) A. Bax, D. G. Davis, *J. Magn. Reson.* **1985**, 65, 355-360; b) C. Griesinger, G. Otting, K. Wüthrich, R. R. Ernst, *J. Am. Chem. Soc.* **1988**, 110, 7870-7872.
- [29] a) C. Bauer, R. Freeman, T. Frenkiel, J. Keeler, A. Shaka, *J. Magn. Reson.* **1984**, 58, 442-457; b) L. Emsley, G. Bodenhausen, *J. Magn. Reson.* **1989**, 82, 211-221.
- [30] A. Bax, R. H. Griffey, B. L. Hawkins, *J. Magn. Reson.* **1983**, 55, 301-315.
- [31] A. Bax, S. Subramanian, *J. Magn. Reson.* **1986**, 67, 565-569.
- [32] A. Bax, M. F. Summers, *J. Am. Chem. Soc.* **1986**, 108, 2093-2094.
- [33] XEASY-ETH Automated Spectroscopy 1.4 (version 60801000 of the XWindow System).
- [34] C. D. Schwieters, J. J. Kuszewski, N. Tjandra, G. M. Clore, *J. Magn. Reson.*, **2003**, 160, 66-74. Based on X-PLOR 3.851 by A.T. Brünger.
- [35] R. Koradi, M. Billeter, K. Wüthrich, *J. Mol. Graphics* **1996**, 14, 51-55.

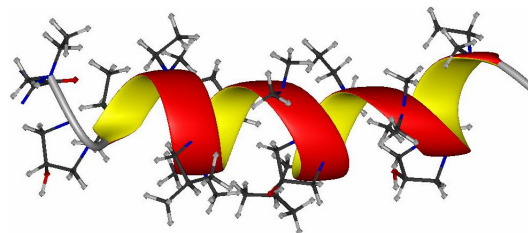
Received: ((will be filled in by the editorial staff))
Revised: ((will be filled in by the editorial staff))
Published online: ((will be filled in by the editorial staff))

Entry for the Table of Contents

Catch Phrase

*M. De Zotti, F. Damato, F. Formaggio, M. Crisma, E. Schievano, S. Mammi, B. Kaptein, Q.B. Broxterman, P.J. Felock, D.J. Hazuda, S.B. Singh, J. Kirschbaum, H. Brückner, C. Toniolo**
..... Page – Page

Total Synthesis, Characterization, and Conformational Analysis of the Naturally-Occurring Hexadecapeptide Integramide A and Its Diastereomer at Positions 14 and 15



A peptide inhibitor of HIV-1 integrase: total synthesis, extensive characterization, and detailed conformational analysis (using CD, FT-IR absorption, 2D NMR, and X-ray diffraction techniques) of the 16-mer peptide integramide A and

selected segments thereof were carried out, providing valuable information aimed at a deeper understanding of the mode of interaction of integramide A with its target enzyme.

Total Synthesis, Characterization, and Conformational Analysis of the Naturally-Occurring Hexadecapeptide Integramide A and Its Diastereomer at Positions 14 and 15

Marta De Zotti,^[1] Francesca Damato,^[1] Fernando Formaggio,^[1] Marco Crisma,^[1] Elisabetta Schievano,^[1] Stefano Mammi,^[1] Bernard Kaptein,^[2] Quirinus B. Broxterman,^[2] Peter J. Felock,^[3] Daria J. Hazuda,^[3] Sheo B. Singh,^[3] Jochen Kirschbaum,^[4] Hans Brückner,^[4] and Claudio Toniolo*^[1]

[1] Institute of Biomolecular Chemistry, CNR, Padova Unit, Department of Chemistry, University of Padova, via Marzolo 1, 35131 Padova, Italy

[2] DSM Pharmaceutical Products, Innovative Synthesis and Catalysis, P.O. Box 18, 6160 MD Geleen, The Netherlands

[3] Merck Research Laboratories, Rahway, NJ 07065 and West Point, PA 19486, U.S.A.

[4] Department of Food Sciences, Interdisciplinary Research Centre for Biosystems, Land Use and Nutrition, University of Giessen, 35392 Giessen, Germany

SUPPORTING INFORMATION

Peptide synthesis and characterization

The syntheses and characterizations of Ac-D-Iva-OH,^{S1} Z-(Aib)₂-OtBu,^{S2} and Z-(Aib)₃-OtBu,^{S3} have already been published.

Segment B

Z-L-Leu-(Aib)₃-OtBu. M.p.: 189-190 °C (from EtOAc, ethyl acetate / PE, petroleum ether). $[\alpha]_{365}^{20}$: -28.3° (*c* = 0.5, MeOH, methanol). IR (KBr): 3371, 3341, 1733, 1708, 1677, 1667, 1530, 1520 cm⁻¹. ¹H NMR (200 MHz, CDCl₃): δ 7.35 (m, 5H, Z-phenyl CH); ; 7.06, 6.70, 6.30 (3s, 3H, 3 NH); 5.12 (s, 3H, Z-CH₂ and 1 NH); 3.96 (m, 1H, α-CH Leu); 1.71-1.58 (m, 3H, β-CH₂ and γ-CH Leu); 1.47 (s, 18H, 6 βCH₃ Aib); 1.43 (s, 9H, 3 CH₃ OtBu); 0.98-0.96 (m, 6H, 2 δ-CH₃ Leu).

Z-L-Iva-L-Leu-(Aib)₃-OtBu. M.p.: 98-99 °C (from EtOAc/PE). $[\alpha]_{D}^{20}$: -35.4° (*c* = 0.4, MeOH). IR (KBr): 3440, 3434, 3347, 3317, 1733, 1690, 1668, 1635, 1536 cm⁻¹. ¹H NMR (200 MHz, CDCl₃): δ 7.37 (m, 5H, Z-phenyl CH); 7.20, 7.16, 6.81 (3s, 3H, 3 NH); 6.30-6.28 (d, 1H, 1 NH); 5.21-5.03 (q, 3H, Z-CH₂ and 1 NH); 3.99 (m, 1H, α-CH Leu); 2.00-1.66 (m, 5H, β-CH₂ Iva, β-CH₂ and γ-CH Leu); 1.54, 1.52, 1.50, 1.48 (4s, 21H, 6 βCH₃ Aib and β-CH₃ Iva); 1.43 (s, 9H, 3 CH₃ OtBu); 0.96-0.85 (m, 9H, 2 δ-CH₃ Leu and γ-CH₃ Iva). MS (ESI-TOF): $[M+H]^+_{\text{calcd}} = 676.95$; $[M+H]^+_{\text{exp}} = 676.44$.

Z-L-Ile-L-Iva-L-Leu-(Aib)₃-OtBu. M.p.: 82-83 °C (from EtOAc/PE). $[\alpha]_{D}^{20}$: -10.6° (*c* = 0.5, MeOH). IR (KBr): 3326, 1729, 1661, 1533 cm⁻¹. ¹H NMR (400 MHz, CDCl₃): δ 7.38 (m, 5H, Z-phenyl CH); 7.15-7.14 (d, 1H, 1 NH); 7.58, 7.32, 6.87, 6.34, 5.25 (5s, 5H, 5 NH); 5.18-5.09 (q, 2H, Z-CH₂); 4.07-4.02 (m, 1H, α-CH Leu); 3.88-3.86 (m, 1H, α-CH Ile); 1.84-1.68 (m, 7H, β-CH₂ Iva, β-CH₂ and γ-CH Leu, β-CH and 1 γ-CH Ile); 1.52, 1.51, 1.48 and 1.46 (4s, 21H, 6 βCH₃ Aib and β-CH₃ Iva); 1.44 (s, 9H, 3 CH₃ OtBu); 1.26 (m, 1H, 1 γ-CH Ile); 1.01-0.82 (m, 12H, 2 δ-CH₃ Leu, γ-CH₃ and δ-CH₃ Ile); 0.85-0.77 (t, 3H, γ-CH₃ Iva).

Z-L-Hyp-L-Ile-L-Iva-L-Leu-(Aib)₃-OtBu. M.p.: 103-105 °C (from EtOAc/PE). $[\alpha]_{D}^{20}$: -37.4° (*c* = 0.5, MeOH). IR (KBr): 3334, 1730, 1662, 1530 cm⁻¹. ¹H NMR (200 MHz, CDCl₃): δ 7.37 (m, 5H, Z-phenyl CH); 7.63, 7.31, 7.28, 7.25, 6.98 (5s, 5H, 5 NH); 7.14-7.11 (d, 1H, 1 NH); 5.28-5.08 (q, 2H, Z-CH₂); 4.37-4.26 (m, 2H, α-CH and γ-CH di Hyp); 4.18-4.07 (m, 2H, α-CH Ile and α-CH Leu); 3.91-3.73 (m, 2H, δ-CH₂ Hyp); 2.19-2.17 (m, 2H, β-CH₂ Hyp); 2.06-2.04 (m, 2H, γ-CH Leu and β-CH Ile); 1.75-1.48 (m, 7H, β-CH₂ Leu, β-CH₂ and β-CH₃ Iva); 1.50, 1.47 (2s, 18H, 6 β-CH₃ Aib); 1.43 (s, 9H, 3

CH₃ OtBu); 1.30-1.23 (m, 3H, δ-CH₃ Ile); 0.98-0.82 (m, 14H, 2 δ-CH₃ Leu, γ-CH₃ Iva, γ-CH₃ and γ-CH₂ Ile).

Z-L-Hyp-L-Ile-L-Iva-L-Leu-(Aib)₃-OH. M.p.: 181-183 °C (from EtOAc/PE). $[\alpha]_D^{20}$: -31.1° (*c* = 0.5, MeOH). IR (KBr): 3323, 1787, 1660, 1532 cm⁻¹. ¹H NMR (200 MHz, CDCl₃/DMSO-*d*₆): δ 7.65-7.63 (m, 2H, 2 NH); 7.36 (m, 5H, Z-phenyl CH); 7.23, 7.22, 7.20, 7.07 (4s, 4H, 4 NH); 5.00 (m, 2H, Z-CH₂); 4.52-4.25 (m, 2H, α-CH and γ-CH Hyp); 3.91 (m, 1H, α-CH); 3.89 (m, 1H, α-CH); 3.75 (m, 2H, δ-CH₂ Hyp); 2.45-2.43 (m, 1H); 1.87-1.84 (m, 2H); 1.31 (s); 1.11 (m); 0.76 (m). MS (ESI-TOF): $[M+H]^+_{\text{calcd}} = 846.49$; $[M+H]^+_{\text{exp}} = 846.47$; $[M+Na]^+_{\text{exp}} = 868.47$.

Segment C

Z-L-Iva-Aib-OtBu. M.p.: 107-108 °C (from EtOAc/PE). $[\alpha]_{365}^{20}$: +5.9° (*c* = 0.5, MeOH). IR (KBr): 3398, 3389, 3300, 1739, 1718, 1658, 1530 cm⁻¹. ¹H NMR (200 MHz, CDCl₃): δ 7.36-7.35 (m, 5H, Z-phenyl CH); 6.75, 5.73 (2s, 2H, 2 NH); 5.09 (s, 2H, Z-CH₂); 2.17, 1.76-1.61 (2m, 2H, β-CH₂ Iva); 1.54, 1.52, 1.50 (3s, 9H, 2 β-CH₃ Aib and β-CH₃ Iva); 1.46 (s, 9H, 3 CH₃ OtBu); 0.90-0.80 (t, 3H γ-CH₃ Iva).

Z-L-Leu-L-Iva-Aib-OtBu. M.p.: 118-119 °C (from EtOAc/PE). $[\alpha]_D^{20}$: -18.9° (*c* = 0.5, MeOH). IR (KBr) 3396, 3380, 1717, 1707, 1680, 1649, 1532 cm⁻¹. ¹H NMR (200 MHz, CDCl₃): δ 7.36-7.32 (m, 5H, Z-phenyl CH); 6.86, 6.76 (2s, 2H, 2 NH); 5.18 (d, 1H, 1 NH); 5.11 (s, 2H, Z-CH₂); 4.17-4.07 (m, 1H, α-CH Leu); 2.44-2.32 (m, 2H, β-CH₂ Iva), 1.74-1.64 (m, 3H, β-CH₂ and γ-CH Leu); 1.54, 1.52 (2s, 9H, 2 β-CH₃ Aib and β-CH₃ Iva); 1.46 (s, 9H, 3 CH₃ OtBu); 0.96-0.93 (d, 6H, 2 δ-CH₃ Leu); 0.82-0.75 (t, 3H γ-CH₃ Iva).

Z-L-Hyp-L-Leu-L-Iva-Aib-OtBu. M.p.: 80-82 °C (from EtOAc/PE). $[\alpha]_D^{20}$: -57.1° (*c* = 0.5; MeOH). IR (KBr) : 3404, 3351, 1723, 1702, 1672, 1526 cm⁻¹. ¹H NMR (200 MHz, CDCl₃): δ 7.34 (m, 5H, Z-phenyl CH); 7.34, 7.05, 6.93 (3s, 3H, 3 NH); 5.15 (m, 2H, Z-CH₂); 4.49-4.28 (m, 2H, α-CH and γ-CH Hyp); 3.62 (m, 2H, δ-CH₂ Hyp); 2.70 (m, 5H, β-CH₂ and γ-CH Leu, and β-CH₂ Iva); 1.60 (m, 2H, β-CH₂ Hyp); 1.51, 1.49 (2s, 9H, 2 β-CH₃ Aib and β-CH₃ Iva); 1.45 (s, 9H, 3 CH₃ OtBu); 0.88-0.75 (m, 9H, γ-CH₃ Iva and 2 δ-CH₃ Leu).

Z-L-Hyp-L-Leu-L-Iva-Aib-OH. M.p.: 85-87 °C (from EtOAc/PE). $[\alpha]_D^{20}$: -62.6° (*c* = 0.5; MeOH). IR (KBr): 3345, 1671, 1528 cm⁻¹. ¹H NMR (200 MHz, CDCl₃): δ 7.35 (m, 5H, Z-phenyl); 7.35-7.28 (m,

2H, 2 NH); 7.14 (s, 1H, NH); 5.15 (q, 2H, Z-CH₂); 4.56-4.53 (m, 2H, α-CH and γ-CH Hyp); 4.09 (m, 1H, α-CH Leu); 3.66-3.63 (m, 2H, δ-CH₂ Hyp); 2.67-1.87 (m, 7H, β-CH₂ Iva, β-CH₂ Hyp, β-CH₂ and γ-CH Leu); 1.56, 1.53, 1.44 (3s, 9H, 2 β-CH₃ Aib and β-CH₃ Iva); 0.94- 0.86 (m, 9H, γ-CH₃ Iva and 2 δ-CH₃ Leu).

Segments D

Z-L-Iva-Gly-OtBu. M.p.: 96-98 °C (from EtOAc/PE). $[\alpha]_{365}^{20}$: +4.8° (*c* = 0.5, MeOH). IR (KBr): 3374, 3313, 1728, 1711, 1644, 1534 cm⁻¹. ¹H NMR (200 MHz, CDCl₃): δ 7.38-7.31 (m, 5H, Z-phenyl CH); 6.56 (t, 1H, 1 NH); 5.57 (s, 1H, 1 NH); 5.09 (s, 2H, Z-CH₂); 3.93-3.90 (m, 2H, α-CH₂ Gly); 2.17, 1.85-1.71 (2m, 2H, β-CH₂ Iva); 1.55 (s, 3H, β-CH₃ Iva); 1.47 (s, 9H, 3 CH₃ OtBu); 0.89-0.82 (t, 3H γ-CH₃ Iva).

Z-D-Iva-Gly-OtBu. M.p.: 95-97 °C (from EtOAc/PE). $[\alpha]_{365}^{20}$: -4.7° (*c* = 0.5, MeOH). IR (KBr): 3374, 3314, 1725, 1711, 1644, 1535 cm⁻¹. ¹H NMR (200 MHz, CDCl₃): δ 7.38-7.30 (m, 5H, Z-phenyl CH); 6.52 (t, 1H, 1 NH), 5.55 (s, 1H, 1 NH); 5.09 (s, 2H, Z-CH₂); 3.94-3.92 (d, 2H, α-CH₂ Gly); 2.18-2.16, 1.89-1.70 (2m, 2H, β-CH₂ Iva); 1.56 (s, 3H, β-CH₃ Iva); 1.47 (s, 9H, 3 CH₃ OtBu); 0.89-0.82 (t, 3H, γ-CH₃ Iva).

Z-D-Iva-L-Iva-Gly-OtBu. M.p.: 119-121 °C (from EtOAc/PE). $[\alpha]_{365}^{20}$: +7.2° (*c* = 0.5, MeOH). IR (KBr): 3353, 3285, 1746, 1701, 1670, 1534 cm⁻¹. ¹H NMR (200 MHz, CDCl₃): δ 7.35 (m, 5H, Z-phenyl CH); 6.89 (t, 1H, 1 NH); 6.73, 5.39 (2s, 2H, 2 NH); 5.09 (s, 2H, Z-CH₂); 3.94-3.88 (t, 2H, α-CH₂ Gly) 2.19-1.76 (2m, 4H, 2 β-CH₂ Iva); 1.53 (s, 3H, β-CH₃ Iva); 1.50 (s, 3H, β-CH₃ Iva); 1.47 (s, 9H, 3 CH₃ OtBu); 0.91-0.79 (m, 6H, 2 γ-CH₃ Iva).

Z-L-Iva-D-Iva-Gly-OtBu. M.p.: 119-120 °C (from EtOAc/PE). $[\alpha]_{365}^{20}$: -7.0° (*c* = 0.5, MeOH). IR (KBr): 3355, 3284, 1746, 1701, 1672, 1535 cm⁻¹. ¹H NMR (400 MHz, CDCl₃): δ 7.36-7.31 (m, 5H, Z-phenyl CH); 6.88 (t, 1H, 1 NH); 6.72 and 5.38 (2s, 2H, 2 NH); 5.09 (s, 2H, Z-CH₂); 3.99-3.84 (m, 2H, α-CH₂ Gly) 2.17-1.99 (2m, 2H, β-CH₂ Iva); 1.87-1.79 (m, 2H, β-CH₂ Iva); 1.53 (s, 3H, β-CH₃ Iva); 1.50 (s, 3H, β-CH₃ Iva); 1.47 (s, 9H, 3 CH₃ OtBu); 0.89-0.81 (m, 6H, 2 γ-CH₃ Iva).

Z-L-Hyp-D-Iva-L-Iva-Gly-OtBu. M.p.: 173-174 °C (from EtOAc/PE). $[\alpha]_{D}^{20}$: -45.7° (*c* = 0.4, MeOH). IR (KBr): 3408, 3370, 1744, 1685, 1671, 1655, 1551 cm⁻¹. ¹H NMR (400 MHz, CDCl₃): δ 7.35 (m, 5H,

Z-phenyl CH); 7.19 (t, 1H, 1 NH Gly); 6.85, 6.74 (2s, 2H, 2 NH); 5.16 (m, 2H, Z-CH₂); 4.54, 4.37 (2m, 2H, α-CH and γ-CH Hyp); 4.01-3.77 (m, 2H); 3.68-3.57 (m, 2H); 2.29-1.83 (m, 6H, 2 β-CH₂ Iva and β-CH₂ Hyp); 1.44 (s, 15H, 2 β-CH₃ Iva and 3 CH₃ OtBu); 0.89-0.81 (m, 6H, 2 γ-CH₃ Iva). MS (ESI-TOF): [M+H]⁺_{calcd} = 577.32; [M+H]⁺_{exp} = 577.28; [M+Na]⁺_{exp} = 599.27.

Z-L-Hyp-L-Iva-D-Iva-Gly-OtBu. M.p.: 167-169 °C (from EtOAc/PE). [α]²⁰_D: -46.0° (c = 0.5, MeOH). IR (KBr): 3378, 1744, 1676, 1539 cm⁻¹. ¹H NMR (400 MHz, CDCl₃): δ 7.36 (m, 5H, Z-phenyl CH); 7.16 (t, 1H, 1 NH Gly); 6.89, 6.77 (2s, 2H, 2 NH); 5.16 (s, 2H, Z-CH₂); 4.54 (m, 1H, γ-CH Hyp); 4.45-4.37 (m, 1H, α-CH Hyp); 3.95-3.85 (m, 2H, α-CH₂ Gly); 3.72-3.61 (m, 2H, δ-CH₂ Hyp); 2.26-1.81 (m, 6H, 2 β-CH₂ Iva and β-CH₂ Hyp); 1.52 (s, 3H, β-CH₃ Iva); 1.46-1.42 (2s, 12H, β-CH₃ Iva and 3 CH₃ OtBu); 0.90-0.77 (m, 6H, 2 γ-CH₃ Iva). MS (ESI-TOF): [M+H]⁺_{calcd} = 577.76; [M+H]⁺_{exp} = 577.34.

Z-L-Hyp-D-Iva-L-Iva-Gly-OH. M.p.: 202-204 °C (from EtOAc/PE). [α]²⁰_D: -43.4° (c = 0.5, MeOH). IR (KBr): 3386, 1744, 1660, 1541 cm⁻¹. ¹H NMR (400 MHz, 10% DMSO-*d*₆ / 90% CDCl₃): δ 7.64, 7.56 (m, 2H, 2 NH) 7.50 (t, 1H, NH Gly); 7.33 (m, 5H, Z-phenyl); 7.06 (s, 1H, NH); 5.18-5.03 (q, 2H, Z-CH₂); 4.43 (m, 2H, α-CH and γ-CH Hyp); 3.90-3.85 (m, 2H, δ-CH₂ Hyp); 3.66-3.26 (q, 2H, α-CH₂ Gly); 2.15-1.78 (m, 6H, 2 β-CH₂ Iva and β-CH₂ Hyp); 1.42, 1.37 (2s, 6H, 2 β-CH₃ Iva); 0.92- 0.89 (t, 3H, γ-CH₃ Iva); 0.92- 0.72 (t, 3H, γ-CH₃ Iva). MS (ESI-TOF): [M+H]⁺_{calcd} = 521.65; [M+H]⁺_{exp} = 521.28; [M+Na]⁺_{exp} = 543.25.

Z-L-Hyp-L-Iva-D-Iva-Gly-OH. M.p.: 200-202 °C (from EtOAc/PE). [α]²⁰_D: -66.0° (c = 0.5, MeOH). IR (KBr): 3394, 1746, 1666, 1549 cm⁻¹. ¹H NMR (400 MHz, 10% DMSO-*d*₆ / 90% CDCl₃): δ 7.84 (s, 1H, 1 NH) 7.58 (t, 1H, NH Gly); 7.33 (m, 5H, Z-phenyl); 7.19 (s, 1H, NH); 5.16-5.05 (q, 2H, Z-CH₂); 4.43-4.42 (m, 2H, α-CH and γ-CH Hyp); 3.95-3.83 (m, 2H, δ-CH₂ Hyp); 3.66-3.54 (q, 2H, α-CH₂ Gly); 2.17-1.72 (4m, 6H, 2 β-CH₂ Iva and β-CH₂ Hyp); 1.46, 1.36 (2s, 6H, 2 β-CH₃ Iva); 0.88- 0.85 (t, 3H, γ-CH₃ Iva); 0.79- 0.75 (t, 3H, γ-CH₃ Iva). MS (ESI-TOF): [M+H]⁺_{calcd} = 521.65; [M+H]⁺_{exp} = 521.27; [M+Na]⁺_{exp} = 543.27.

Segments C-D

Z-L-Hyp-L-Leu-L-Iva-Aib-L-Hyp-D-Iva-L-Iva-Gly-OtBu. M.p.: 108-110 °C (from EtOAc/PE). $[\alpha]_D^{20}$: -17.0° ($c = 0.4$, MeOH). IR (KBr): 3439, 3328, 1746, 1732, 1656, 1535 cm^{-1} . ^1H NMR (400 MHz, CDCl_3): δ 7.82, 7.65 (2s, 2 H, 2 NH); 7.53 (t, 1H, NH Gly); 7.38-7.31 (m, 5H, Z-phenyl CH); 7.23, 7.18, 6.93 (3s, 3H, 3 NH); 5.25 (q, 2H, Z- CH_2); 4.56-4.42 (m, 4H); 4.07-3.97 (m, 1H); 4.01-3.97 (m, 1H); 3.73-3.58 (2m, 5H); 2.40-2.25 (2m, 4H); 2.10-1.60 (4m, 9H); 1.57, 1.52, 1.50, 1.43, 1.38 (5s, 15H, β - CH_3 Aib and β - CH_3 Iva); 1.42 (s, 9H, 3 CH_3 OtBu); 1.03-0.71 (3m, 15H, 3 γ - CH_3 Iva and 2 δ - CH_3 Leu). MS (ESI-TOF): $[\text{M}+\text{H}]^+_{\text{calcd}} = 987.58$; $[\text{M}+\text{H}]^+_{\text{exp}} = 987.51$; $[\text{M}+\text{Na}]^+_{\text{exp}} = 1009.52$.

Z-L-Hyp-L-Leu-L-Iva-Aib-L-Hyp-L-Iva-D-Iva-Gly-OtBu. M.p.: 108-109 °C (from EtOAc/PE). $[\alpha]_D^{20}$: -27.6° ($c = 0.5$, MeOH). IR (KBr): 3331, 1738, 1658, 1640, 1534 cm^{-1} . ^1H NMR (400 MHz, CDCl_3): δ 7.71, 7.55 (2s, 2H, 2 NH); 7.44-7.42 (t, 1H, NH Gly); 7.37-7.33 (m, 5H, Z-phenyl CH); 7.31 (s, 1H, 1 NH); 7.11, 6.97 (2s, 2H, 2NH); 5.16-5.13 (q, 2H, Z- CH_2); 4.52-4.45 (m, 4H, 2 α -CH and 2 γ -CH Hyp); 4.03-3.98 (m, 1H); 3.78-3.61 (m, 6H); 2.38-1.65 (4m, 13H); 1.48, 1.47, 1.44, 1.43 (4s, 24H, 2 β - CH_3 Aib, 3 β - CH_3 Iva and 3 CH_3 OtBu); 0.97-0.76 (m, 15H, 3 γ - CH_3 Iva and 2 δ - CH_3 Leu). MS (ESI-TOF): $[\text{M}+\text{H}]^+_{\text{calcd}} = 987.58$; $[\text{M}+\text{H}]^+_{\text{exp}} = 987.54$; $[\text{M}+\text{Na}]^+_{\text{exp}} = 1009.53$.

Segments B-C-D

Z-L-Hyp-L-Ile-L-Iva-L-Leu-Aib-Aib-Aib-L-Hyp-L-Leu-L-Iva-Aib-L-Hyp-D-Iva-L-Iva-Gly-OtBu. M.p.: 147-149 °C (from EtOAc/PE). $[\alpha]_D^{20}$: -10.3° ($c = 0.5$, MeOH). IR (KBr): 3335, 1748, 1732, 1656, 1535 cm^{-1} . ^1H NMR (600 MHz, CDCl_3): δ 7.92 (m, 2H, 2 NH); 7.85 (d, 1H, 1 NH); 7.39 (m, 5H, Z-phenyl CH); 7.79, 7.65, 7.53, 6.96, 6.86 (5s, 5H, 5 NH); 7.32, 7.25, 7.23 (3m, 5H, 5 NH); 5.27-5.14 (q, 2H, Z- CH_2); 4.56-4.52 (m, 6H, 3 α -CH and 3 γ -CH Hyp); 4.18 (m, 1H); 4.07-4.00 (m, 3H); 3.95 (m, 1H); 3.90-3.88 (d, 1H); 3.78 (m, 4H); 3.71-3.69 (m, 2H); 3.51-3.48 (m, 1H); 2.39-2.37 (m, 4H); 2.07 (m, 1H); 1.98 (m, 2H); 1.90-1.81 (m, 5H); 1.57-1.46 (m, 33H, 3 CH_3 OtBu, 4 β - CH_3 Aib and 4 β - CH_3 Iva); 1.01-0.86 (m, 11H); 0.83-0.71 (m, 3H). MS (ESI-TOF): $[\text{M}]_{\text{calcd}} = 1680.01$; $[\text{M} - \text{B}+\text{H}]^+_{\text{exp}} = 828.55$; $[\text{M} - \text{C-D}+\text{Na}]^+_{\text{exp}} = 853.60$.

Z-L-Hyp-L-Ile-L-Iva-L-Leu-Aib-Aib-Aib-L-Hyp-L-Leu-L-Iva-Aib-L-Hyp-L-Iva-D-Iva-Gly-OtBu. M.p.: 149-151 °C (from EtOAc/PE). $[\alpha]_D^{20}$: -14.3° ($c = 0.5$, MeOH). IR (KBr): 3320, 1740, 1656, 1650, 1535 cm^{-1} . ^1H NMR (600 MHz, CDCl_3): δ 7.88 (d, 1H, 1 NH); 7.80-7.78 (d, 1H, 1 NH); 7.74 (s, 2H, 2 NH); 7.51 (t, 1H, NH Gly); 7.46 (s, 1H, 1 NH); 7.37 (m, 5H, Z-phenyl CH); 7.36-7.31 (bs, 2H, 2 NH); 7.20 (s, 1H, 1 NH); 7.16 (s, 1H, 1 NH); 6.94 (d, 1H, 1 NH); 5.27-5.12 (q, 2H, Z- CH_2); 4.54-4.47 (m, 6H, 3 α -CH and 3 γ -CH Hyp); 4.15-3.68 (4m, 11H); 2.42 (m, 4H); 2.09-1.68 (m, 8H); 1.57-1.46 (m,

33H, 3 CH₃ OtBu, 4 β-CH₃ Aib and 4 β-CH₃ Iva); 1.01-0.86 (m, 11H); 0.83-0.71 (m, 3H). MS (ESI-TOF): [M+H]⁺_{calcd} = 1680.01; [M – B+H]⁺_{exp} = 828.45; [M – C-D+Na]⁺_{exp} = 853.49.

Hexadecapeptides A-B-C-D

Ac-D-Iva-L-Hyp-L-Ile-L-Iva-L-Leu-Aib-Aib-Aib-L-Hyp-L-Leu-L-Iva-Aib-L-Hyp-D-Iva-L-Iva-Gly-OtBu. M.p.: 152-154 °C (from EtOAc/PE). [α]²⁰_D: -7.0° (c = 0.2, MeOH). IR (KBr): 3357, 1734, 1648, 1534 cm⁻¹. ¹H NMR (600 MHz, DMSO-*d*₆): δ 8.82 (s, 1H, NH Iva¹); 7.76 (d, 1H, NH Leu¹⁰); 7.75 (s, 1H, NH Aib⁶); 7.74 (d, 1H, NH Ile³); 7.73 (s, 1H, NH Aib⁸); 7.70 (s, 1H, NH Iva¹⁴); 7.62 (t, 1H, NH Gly¹⁶); 7.56 (s, 1H, NH Aib¹²); 7.32 (s, 1H, NH Aib⁷); 7.19 (d, 1H, NH Leu⁵); 7.12 (s, 1H, NH Iva¹⁵); 7.11 (s, 1H, NH Iva¹¹); 7.02 (s, 1H, NH Iva⁴); 5.17 (s, 1H, Hyp²); 5.10 (s, 1H, Hyp¹³); 5.00 (s, 1H, Hyp⁹); 4.32 (m, 2H, Hyp²); 4.27 (m, 2H, Hyp⁹); 4.24 (m, 2H, Hyp¹³); 3.97 (m, 1H, α-CH Leu¹⁰); 3.92 (m, 1H, α-CH Leu⁵); 3.78 (m, 1H, δ-CH Hyp²); 3.77 (m, 1H, δ-CH Hyp¹³); 3.74 (m, 1H, 1 α-CH Gly¹⁶); 3.64 (m, 1H, δ-CH Hyp⁹); 3.62 (m, 1H, α-CH Ile³); 3.55 (m, 1H, 1 α-CH Gly¹⁶); 3.53 (m, 1H, δ-CH Hyp¹³); 3.52 (m, 1H, δ-CH Hyp⁹); 3.38 (m, 1H, δ-CH Hyp²); 2.17 (m, 2H); 2.08 (m); 1.99 (s, 3H, CH₃ Ac); 1.93 (m, 1H, β-CH Ile³); 1.90 (m, 1H); 1.85-1.70 (m, 13H); 1.68 (m); 1.51 (s); 1.42 (s); 1.41 (s); 1.40 (s); 1.39 (s); 1.37 (s); 1.36 (s); 1.34 (s); 1.28 (s); 1.25 (s); 1.11 (m, 2H, γ-CH₂ Ile³); 0.86-0.67 (m, 30H, γ-CH₃ Iva, δ-CH₃ Leu, γ-CH₃ and δ-CH₃ Ile). MS (ESI-TOF): [M+H]⁺_{calcd} = 1687.14; [M+H]⁺_{exp} = 1686.51.

Ac-D-Iva-L-Hyp-L-Ile-L-Iva-L-Leu-Aib-Aib-Aib-L-Hyp-L-Leu-L-Iva-Aib-L-Hyp-L-Iva-D-Iva-Gly-OtBu. M.p.: 162-164 °C (from EtOAc/PE). IR (KBr): 3336, 1735, 1644, 1536 cm⁻¹. MS (ESI-TOF): [M – C-D+H]⁺_{exp} = 853.51; [M – A-B+H]⁺_{exp} = 835.52.

Ac-D-Iva-L-Hyp-L-Ile-L-Iva-L-Leu-Aib-Aib-Aib-L-Hyp-L-Leu-L-Iva-Aib-L-Hyp-D-Iva-L-Iva-Gly-OH. M.p.: 206-208 °C (from EtOAc/PE). IR (KBr): 3385, 1645, 1535 cm⁻¹. ¹H NMR (600 MHz, , 300K, TFE-*d*₂): δ 8.17 (s, 1H, NH Iva¹⁴); 8.13 (d, 1H, NH Leu¹⁰); 7.90 (s, 2H, NH Aib⁶ and NH Aib⁸); 7.88-7.87 (d, 1H, NH Ile³); 7.77 (t, 1H, NH Gly¹⁶); 7.70 (s, 1H, NH Aib⁷); 7.59 (s, 1H, NH Aib¹²); 7.49 (s, 1H, 1 NH Iva¹⁵); 7.41 (d, 1H, NH Leu⁵); 7.13 (s, 1H, NH Iva¹¹); 7.12 (s, 1H, NH Iva¹); 7.10 (s, 1H, NH Iva⁴); 4.63-4.53 (m, 6H, αCH, γCH Hyp², γCH Hyp⁹ and γCH Hyp¹³); 4.26 (m, 1H, αCH Leu¹⁰); 4.13-3.99 (m, 7H, αCH Leu⁵, αCH₂ Gly¹⁶, δCH₂ Hyp⁹, δCH Hyp² and δCH Hyp¹³); 3.82-3.72 (m, 2H, αCH Ile³ and δCH Hyp²); 3.54-3.52 (m, 1H, δCH Hyp²); 2.41 (m, 3H, βCH Hyp², βCH Hyp⁹ and βCH Hyp¹³); 2.31 (m, 1H, βCH Iva¹⁴); 2.22 (m, 1H, βCH Iva¹); 2.10 (s, 3H, CH₃ Ac); 2.07-2.02 (m, 3H,

β CH Iva⁴, β CH Iva¹⁵ and β CH Ile³); 1.96-1.93 (m, 7H, β CH Hyp⁹, β CH Hyp² and β CH Hyp¹³, β CH Leu¹⁰, β CH Iva¹¹, β CH Iva¹ and β CH Iva¹⁵); 1.88-1.86 (m, 3H, β CH Leu⁵, β CH Iva⁴ and β CH Iva¹¹); 1.76-1.73 (m, 2H, γ CH Leu¹⁰ and β CH Iva¹⁴); 1.68 (s, 4H, β CH Leu¹⁰ and β -CH₃ pro-*S* Aib⁸); 1.66 (s, 3H, β -CH₃ pro-*S* Aib⁷); 1.62 (s, 3H, pro-*R* Aib⁶); 1.60 (s, 4H, γ -CH Ile³ and β CH₃ Iva¹¹); 1.58 (s, 10H, β CH₃ pro-*R* Aib⁷, β CH₃ pro-*S* Aib⁶, β CH₃ pro-*S* Aib¹² and β CH Leu⁵); 1.56 (s, 3H, β CH₃ pro-*R* Aib⁸); 1.52 (s, 9H, β CH₃ pro-*R* Aib¹², β CH₃ Iva⁴ and β CH₃ Iva¹⁴); 1.50 (s, 3H, β CH₃ Iva¹⁵); 1.45 (s, 3H, β CH₃ Iva¹); 1.26-1.22 (m, 1H, γ -CH Ile³); 1.01-0.93 (m, 30H, 2 δ -CH₃ Leu¹⁰, γ -CH₃ Ile³, δ -CH₃ Ile³, γ -CH₃ Iva¹⁵, γ -CH₃ Iva¹¹, γ -CH₃ Iva⁴, γ -CH₃ Iva¹ and 2 δ -CH₃ Leu⁵); 0.88-0.86 (t, 3H, γ -CH₃ Iva¹⁴). MS (ESI-TOF): [M+H]⁺_{calcd} = 1633.02; [M+H]⁺_{exp} = 1633.10; [M+2H]²⁺_{exp} = 816.98; [M+H+Na]²⁺_{exp} = 827.99.

Ac-D-Iva-L-Hyp-L-Ile-L-Iva-L-Leu-Aib-Aib-Aib-L-Hyp-L-Leu-L-Iva-Aib-L-Hyp-L-Iva-D-Iva-Gly-OH. M.p.: 225-227 °C (from EtOAc/PE). IR (KBr): 3422, 1646, 1535 cm⁻¹. ¹H NMR (600 MHz, TFE-*d*₂): δ 8.12 (d, 1H, NH Leu¹⁰); 7.91 (s, 2H, NH Aib⁶ and NH Aib⁸); 7.88-7.87 (d, 1H, NH Ile³); 7.72 (s, 1H, NH Aib⁷); 7.61 (s, 1H, NH Aib¹²); 7.58 (s, 1H, NH Iva¹⁴); 7.43-7.42 (d, 1H, NH Leu⁵); 7.21 (t, 1H, NH Gly¹⁶); 7.17 (s, 1H, NH Iva¹¹); 7.14 (s, 2H, NH Iva¹⁵ and NH Iva¹); 7.12 (s, 1H, NH Iva⁴); 4.65 (m, 1H, γ -CH Hyp¹³); 4.62-4.57 (m, 4H, γ -CH Hyp⁹, α -CH Hyp⁹, γ -CH Hyp², α -CH Hyp²); 4.48-4.45 (t, 1H, α -CH Hyp¹³); 4.26 (m, 1H, α -CH Leu¹⁰); 4.13 (m, 1H, α -CH Leu⁵); 4.07-4.06 (2m, 1H, δ CH Hyp⁹); 4.02-3.99 (2m, 1H, δ CH Hyp²); 3.92-3.90 (m, 3H, δ CH Hyp⁹, δ CH Hyp¹³, α -CH Gly¹⁶); 3.82-3.77 (m, 2H, α -CH Ile³ and α -CH Gly¹⁶); 3.74-3.72 (2m, 1H, δ CH Hyp¹³); 3.54-3.53 (2m, 1H, δ CH Hyp²); 2.44-2.41 (m, 2H, β -CH Hyp² and β -CH Hyp⁹); 2.35 (m, 1H, β -CH Hyp¹³); 2.25-2.22 (m, 1H, β -CH Iva¹); 2.16 (m, 1H, β -CH Iva¹⁴); 2.11 (s, 4H, CH₃ Ac and β -CH Iva¹⁵); 2.09-2.05 (m, 2H, β -CH Ile³ and β -CH Iva⁴); 1.99-1.93 (m, 6H, β -CH Hyp⁹, β -CH Iva¹, β -CH Iva¹¹, β -CH Hyp², β -CH Leu¹⁰ and β -CH Hyp¹³); 1.89-1.85 (m, 6H, β -CH Iva¹⁴, β -CH₂ Leu⁵, β -CH Iva¹¹, β -CH Iva¹⁵ and β -CH Iva⁴); 1.76-1.70 (m, 2H, β -CH and γ -CH Leu¹⁰); 1.68 (s, 3H, pro-*R* β -CH₃ Aib⁸); 1.66 (s, 3H, pro-*R* β -CH₃ Aib⁷); 1.63 (s, 3H, pro-*S* β -CH₃ Aib⁶); 1.61 (m, 1H, γ -CH Ile³); 1.58 (s, 9H, pro-*S* β -CH₃ Aib⁷, pro-*R* β -CH₃ Aib⁶ and β -CH₃ Iva¹¹); 1.58 (s, 3H, pro-*R* β -CH₃ Aib¹²); 1.57 (s, 4H, γ -CH Leu⁵ and pro-*S* β -CH₃ Aib⁸); 1.52 (s, 6H, β -CH₃ Iva⁴ and β -CH₃ Iva¹⁵); 1.49 (s, 6H, pro-*S* β -CH₃ Aib¹² and β -CH₃ Iva¹⁴); 1.45 (s, 3H, β -CH₃ Iva¹); 1.27-1.19 (m, 1H, γ -CH Ile³); 1.01-0.99 (m, 9H, δ -CH₃ Leu¹⁰, γ -CH₃ Iva⁴ and γ -CH₃ Ile³); 0.98-0.93 (m, 21H, 2 δ -CH₃ Leu⁵, δ -CH₃ Leu¹⁰, γ -CH₃ Iva¹, γ -CH₃ Iva¹¹, γ -CH₃ Iva¹⁴ and δ CH₃ Ile³); 0.90-0.89 (t, 3H, γ CH₃ Iva¹⁵). MS (ESI-TOF): [M+Na]⁺_{calcd} = 1655.02; [M+Na]⁺_{exp} = 1655.08; [M+2Na]²⁺_{exp} = 838.96; [M+2H]²⁺_{exp} = 816.98; [M+H+Na]²⁺_{exp} = 827.99.

Supporting References

- (S1) Crisma, M.; Valle, G.; Formaggio, F.; Toniolo, C.; Broxterman, Q. B.; Kamphuis, J. *Zeit. Kristallogr. (NCS)* **1998**, *213*, 313.
- (S2) Leibfritz, D.; Haupt, E.; Dubischar, N.; Lachmann, H.; Oekonomopulos, R.; Jung, G. *Tetrahedron* **1982**, *38*, 2165.
- (S3) Jones, D. S.; Kenner, G. W.; Preston, J.; Sheppard, R. C. *J. Chem. Soc.* **1965**, 6227.

Table S1. Intra- and Intermolecular H-bond Parameters (\AA , $^\circ$) for the X-ray Diffraction Structures Described in This Work

D-H...A	d(D-H)	d(H...A)	d(D...A)	$\angle(\text{DHA})$	Symmetry equiv. of A
<i>Z-L-Hyp-L-Iva-D-Iva-Gly-OtBu</i>					
N3-H3...O0	0.86	2.45	3.134(5)	137.5	x, y, z
N4-H4...O1	0.86	2.46	3.239(5)	151.8	x, y, z
N2-H2...O	0.86	2.06	2.903(4)	166.8	-x+1, y+1/2, -z+3/2
O1G-H1G1...O1	0.82	1.92	2.666(4)	151.3	-x, y+1/2, -z+3/2
<i>Z-L-Iva-L-Leu-(Aib)₃-OtBu</i>					
N3-H3...O0	0.86	2.10	2.949(8)	168.5	x, y, z
N4-H4...O1	0.86	2.32	3.148(9)	161.7	x, y, z
N5-H5...O2	0.86	2.14	2.953(9)	157.9	x, y, z
N1-H1...O4	0.86	2.03	2.889(9)	176.6	x, y, z+1
<i>Z-L-Ile-L-Iva-L-Leu-(Aib)₃-OtBu</i>					
N3-H3...O0	0.86	2.51	3.230(9)	141.3	x, y, z
N4-H4...O1	0.86	2.25	3.063(8)	157.7	x, y, z
N5-H5...O2	0.86	2.22	3.024(9)	156.1	x, y, z
N6-H6...O3	0.86	2.31	3.124(9)	157.5	x, y, z
N1-H1...O4	0.86	2.08	2.934(8)	176.6	x-1/2, y-1/2, z
N2-H2...O51	0.86	2.58	3.374(10)	153.2	x-1/2, y-1/2, z

Table S2. Proton Chemical Shift Assignment for Integramide A (1.45 mM in TFE-*d*₂, T = 300 K)^a

residue	HN	α H	β H	β' H	γ H	δ H
Ac		2.103				
D-Iva ¹	7.126		2.233 1.966	1.447	0.936	
L-Hyp ²		4.584	1.955	2.448	4.576	3.5324.001
L-Ile ³	7.878	3.805	2.077		1.246 1.613	0.969
					0.996	
L-Iva ⁴	7.121		2.066 1.866	1.522	0.953	
L-Leu ⁵	7.416	4.128	1.573	1.886	1.876	0.943 0.921
Aib ⁶	7.907		1.579	1.629		
Aib ⁷	7.707		1.657	1.580		
Aib ⁸	7.904		1.684	1.569		
L-Hyp ⁹		4.604	1.978	2.410	4.609	3.917 4.051
L-Leu ¹⁰	8.122	4.262	1.703	1.977	1.766	1.007 0.940
L-Iva ¹¹	7.134		1.948 1.854	1.596	0.980	
Aib ¹²	7.572		1.573	1.512		
L-Hyp ¹³		4.519	1.925	2.395	4.642	3.773 3.940
Iva ¹⁴	8.071		2.087 1.934	1.513	1.010	
Iva ¹⁵	7.626		2.266 1.842	1.527	0.867	
Gly ¹⁶	7.692	4.045 4.082				

^aThe stereospecific assignment of β -protons was achieved only for the two diastereotopic methyls of the Aib residues.

Table S3. Chemical Shifts of $^{13}\text{C}_\beta$ of Methyl Groups of the Aib Residues of Integramide A and the Corresponding CNE Values

residue	$\delta\text{C}_\beta\text{H}_3$ (ppm)	$\delta\text{C}_\beta\text{H}_3$ (ppm)	CNE (ppm)
Aib ⁶	26.70	23.44	3.26
Aib ⁷	28.25	23.37	4.88
Aib ⁸	26.40	24.40	2.00
Aib ¹²	26.17	24.16	2.01

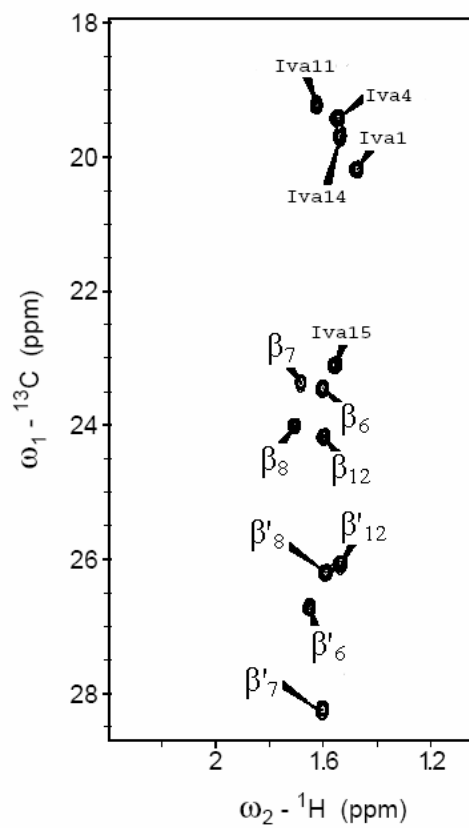


Figure S1. $C\beta$ -Selective HMQC spectrum (600 MHz) of integramide A (1.45 mM in TFE- d_2 , 300K)